

Transcriptome-Wide Changes in *Chlamydomonas reinhardtii* Gene Expression Regulated by Carbon Dioxide and the CO₂-Concentrating Mechanism Regulator CIA5/CCM1

Wei Fang,^a Yaqing Si,^b Stephen Douglass,^{c,d} David Casero,^{c,d} Sabeeha S. Merchant,^{d,e} Matteo Pellegrini,^{c,d} Istvan Ladunga,^f Peng Liu,^b and Martin H. Spalding^{a,1}

^aDepartment of Genetics, Development, and Cell Biology, Iowa State University, Ames, Iowa 50011-3260

^bDepartment of Statistics, Iowa State University, Ames, Iowa 50011-1210

^cDepartment of Molecular, Cell, and Developmental Biology, University of California, Los Angeles, California 90095-1606

^dInstitute of Genomics and Proteomics, University of California, Los Angeles, California 90095-1569

^eDepartment of Chemistry and Biochemistry, University of California, Los Angeles, California 90095-1569

^fDepartment of Statistics, University of Nebraska, Lincoln, Nebraska 68588-0665

We used RNA sequencing to query the *Chlamydomonas reinhardtii* transcriptome for regulation by CO₂ and by the transcription regulator CIA5 (CCM1). Both CO₂ and CIA5 are known to play roles in acclimation to low CO₂ and in induction of an essential CO₂-concentrating mechanism (CCM), but less is known about their interaction and impact on the whole transcriptome. Our comparison of the transcriptome of a wild type versus a *cia5* mutant strain under three different CO₂ conditions, high CO₂ (5%), low CO₂ (0.03 to 0.05%), and very low CO₂ (<0.02%), provided an entry into global changes in the gene expression patterns occurring in response to the interaction between CO₂ and CIA5. We observed a massive impact of CIA5 and CO₂ on the transcriptome, affecting almost 25% of all *Chlamydomonas* genes, and we discovered an array of gene clusters with distinctive expression patterns that provide insight into the regulatory interaction between CIA5 and CO₂. Several individual clusters respond primarily to either CIA5 or CO₂, providing access to genes regulated by one factor but decoupled from the other. Three distinct clusters clearly associated with CCM-related genes may represent a rich source of candidates for new CCM components, including a small cluster of genes encoding putative inorganic carbon transporters.

INTRODUCTION

The photosynthetic conversion of inorganic carbon (C_i) into organic form is responsible for the abundance of biomass on earth. In this process, ribulose-1,5-bis-phosphate carboxylase/oxygenase (Rubisco) catalyzes the initial incorporation of CO₂ via the carboxylation of ribulose biphosphate by CO₂ (reviewed in Andersson, 2008). Although critically important, the catalytic activity of Rubisco is slow compared with many other enzymes and also cannot discriminate completely between CO₂ and O₂; the oxygenation of ribulose biphosphate is competitive with the carboxylation reaction. Under present atmospheric conditions, CO₂ assimilation rates often are limited by the CO₂ concentration, and in many photosynthetic species, ranging from cyanobacteria and algae to C₄ vascular plants, an active CO₂-concentrating mechanism (CCM) has evolved to help offset the deficiencies of Rubisco (Raven et al., 2008). CCMs are especially prevalent in aquatic photosynthetic organisms.

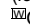
Chlamydomonas reinhardtii, a unicellular green alga that serves as a reference organism, also exhibits acclimations to varied CO₂ levels (reviewed in Spalding, 2009). *C. reinhardtii* must overcome the 10,000-fold slower diffusion of CO₂ in water relative to air. Thus, active transport and accumulation of C_i, either as CO₂ or as HCO₃[−], plays a critical role in the *C. reinhardtii* CCM (Moroney and Ynalvez, 2007; Spalding, 2008). Internal accumulation of C_i occurs against a large concentration gradient, so accumulation must occur as HCO₃[−] because its permeability across lipid membranes is 1000-fold lower than that of CO₂. However, Rubisco uses CO₂ as substrate, so, along with C_i transporters, carbonic anhydrases (CAs), which catalyze interconversion of CO₂ and HCO₃[−], also play important roles in the CCM, (Spalding et al., 1983a; Coleman and Grossman, 1984; Moroney et al., 2011).

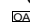
The *C. reinhardtii* CCM is induced by low CO₂ concentrations, and the discovery of CCM-related genes has been based on identifying genes with elevated expression under limiting CO₂ (lower than 0.05%) compared with high CO₂ (1 to 5% CO₂) (Spalding and Jeffrey, 1989; Chen et al., 1997; Somanchi and Moroney, 1999; Miura et al., 2004; Yamano and Fukuzawa, 2009). Many CAs and putative transporters or other LCI (for low CO₂ inducible) genes have been discovered by this criterion and have been hypothesized to relate to the CCM of *C. reinhardtii* (Miura et al., 2004; Yamano and Fukuzawa, 2009).

The detailed regulatory mechanisms of the CCM remain unclear, but two important transcription regulators have been

¹ Address correspondence to mspaldin@iastate.edu.

The authors responsible for distribution of materials integral to the findings presented in this article in accordance with the policy described in the Instructions for Authors (www.plantcell.org) are: Wei Fang (fangwei@iastate.edu) and Martin H. Spalding (mspaldin@iastate.edu).

 Online version contains Web-only data.

 Open Access articles can be viewed online without a subscription.
www.plantcell.org/cgi/doi/10.1105/tpc.112.097949

identified and characterized based on their relationship to the CCM. A zinc-finger type transcription regulator, CIA5 (or CCM1), was identified by complementation of the *cia5* mutant (Moroney et al., 1989), which is unable to acclimate to limiting CO₂ conditions, and, independently, by cloning of a tagged allele of *cia5*, *ccm1* (Fukuzawa et al., 2001; Xiang et al., 2001). Expression of most putative C_i transporters and induced CAs requires CIA5, even though the expression of CIA5 itself does not depend on the CO₂ level, so posttranslational activation of CIA5 in low CO₂ apparently is required for CIA5 to regulate these genes (Fukuzawa et al., 2001; Xiang et al., 2001; Miura et al., 2004). Another transcription regulator, low-CO₂ response regulator1 (LCR1), has a Myb domain and appears to regulate the expression of at least three limiting CO₂ induced genes, *carbonic anhydrase1* (CAH1), *low-CO₂-induced gene1* (LCI1), and *LCI6*. *LCR1* itself also is induced by limiting CO₂, and this induction requires Ci accumulation5 (CIA5) (Yoshioka et al., 2004). Because of the extensive connection of CIA5 to regulation of the CCM-related genes, including LCR1, CIA5 is often called the master regulator of the CCM.

Regarding the mechanism of C_i transport and accumulation in the CCM, the first barrier to C_i uptake is the plasma membrane. Two CIA5-regulated genes encoding candidate transporters have been implicated in C_i transport across the plasma membrane: *high light-induced gene3* (HLA3) encodes a putative ATP binding cassette type transporter and is induced under low CO₂ conditions, and knockdown of its expression impairs photosynthesis, C_i uptake, and growth in alkaline conditions (Duanmu et al., 2009a). *LCI1* encodes a plasma membrane protein reported to increase C_i uptake in LCR1 mutants when expressed transgenically (Ohnishi et al., 2010). Two Rhesus-like proteins, RHP1 and RHP2, also are predicted to be plasma membrane located (Yoshihara et al., 2008). The RHP1 protein has been proposed as a CO₂ channel to facilitate CO₂ influx under high CO₂ conditions (Soupene et al., 2002, 2004), and its expression is reportedly upregulated in high CO₂.

Some chloroplast envelope proteins also are candidates to transport C_i into the stroma. The *low CO₂-induced gene A* (LCIA [NAR1.2]) gene, which encodes a Formate/Nitrite Transporter family protein targeted to the chloroplast envelope, is induced in low CO₂ and requires CIA5 for expression (Galván et al., 2002; Miura et al., 2004). *LCIA* has been reported to increase HCO₃⁻ transport when transfected into *Xenopus laevis* oocytes (Mariscal et al., 2006), and its product has been implicated in C_i transport in *HLA3-LCIA* cknockdown *C. reinhardtii* strains (Duanmu et al., 2009a). RNA interference knockdown of *chloroplast carrier protein1* (CCP1) and *CCP2*, which encode nearly identical, LCI chloroplast envelope proteins (Spalding and Jeffrey, 1989; Ramazanov et al., 1993; Chen et al., 1997) resulted in poor growth under low CO₂ conditions, although no direct evidence for a defect in C_i transport or photosynthesis was demonstrated (Pollock et al., 2004).

The combined transport of HCO₃⁻ across the plasma membrane and the chloroplast envelope results in the accumulation of HCO₃⁻ in the chloroplast stroma. Since Rubisco, located in the pyrenoid, cannot use HCO₃⁻, a specific CA, carbonic anhydrase3 (CAH3), dehydrates the accumulated HCO₃⁻ to CO₂ in the thylakoid lumen, taking advantage of the acidic lumen

environment to drive nearly complete conversion of HCO₃⁻ to CO₂ (Spalding, 2008; Moroney et al., 2011). This essential role of CAH3 also mandates the transport or facilitated diffusion of HCO₃⁻ across the thylakoid membrane, but this has not yet been demonstrated.

Another set of low CO₂-induced genes, *low CO₂-induced gene B* (LCIB) and three related genes, *LCIC*, *LCID*, and *LCIE*, also have been implicated in C_i transport and accumulation even though they are predicted to be soluble chloroplast proteins (Wang and Spalding, 2006; Moroney and Ynalvez, 2007; Spalding, 2008). *LCIB* mutants fail to accumulate internal C_i in low CO₂ conditions and are thus unable to grow in air levels of CO₂ (Spalding et al., 1983b; Wang and Spalding, 2006). Notably, *LCIB* mutants have revealed the existence of a third acclimation state at very low CO₂ concentrations (<0.02%): Both *LCIB* allelic mutants *pmp1* and *ad1* die under low CO₂ conditions (<0.05 and >0.02%) but are able to grow slowly under very low CO₂ (<0.02%) conditions (Wang and Spalding, 2006).

Because transmembrane domains are not evident, these LCIB family proteins cannot be stand-alone C_i transporters. It has been suggested that they might serve as C_i transport regulators or as C_i transport complex subunits (Wang and Spalding, 2006), but LCIB either distributes through the stroma or concentrates around the pyrenoid (Duanmu et al., 2009b; Yamano et al., 2010), making interaction with C_i transporters unlikely. Mutants defective in the thylakoid lumen CA, CAH3, suppress the *LCIB* mutation phenotype (Duanmu et al., 2009b), suggesting a role for LCIB and LCIC, with which LCIB forms a heteromeric complex (Yamano et al., 2010), in preventing the leakage of CO₂ from the stroma. CAH6, a putative chloroplast stromal CA, also may be involved in CO₂-to-HCO₃⁻ conversion in the stroma to reduce diffusive loss of CO₂ from the chloroplast (Mitra et al., 2004).

Even though the *C. reinhardtii* CCM has been extensively studied in recent years, we still know little about the limiting CO₂ acclimation process, and the potential for discovery of new genes involved in this process is very high. The acclimation to limiting CO₂ and induction of the CCM in *C. reinhardtii* appear to be regulated by the master regulator, CIA5 (or CCM1) (Miura et al., 2004). The *cia5* mutant appears to completely lack induction of the CCM, although it is viable under high CO₂ conditions and grows more slowly than the wild type in air levels of CO₂. Also, most identified LCI genes remain uninduced when *cia5* is exposed to low CO₂ (Moroney et al., 1989; Spalding et al., 2002). Aside from being a critical upstream regulator of the CCM and other low CO₂ acclimation responses and likely requiring posttranslational activation in low CO₂, the details of CIA5 function remain undiscovered. CIA5 has been proposed to be a transcription regulator (Fukuzawa et al., 2001; Xiang et al., 2001), but we know very little about sequences recognized by its putative DNA binding domain or the genes it directly regulates downstream.

To better understand the CCM and low CO₂ acclimation of *C. reinhardtii* in general, as well as the function of CIA5, we conducted RNA sequencing (RNA-Seq) experiments employing the Illumina Genome Analyzer II because of its superiority over the traditional microarray methods (González-Ballester et al., 2010; Wang et al., 2010; Castruita et al., 2011) using two *C. reinhardtii*

strains: the 137c wild type (cc125) and *cia5* (cc2702), a mutant in the 137c background with a point mutation in *CIA5*. To also gain insight into the multiple acclimation states, the strains were grown at three different CO₂ concentrations as quantified below: high CO₂ (H-CO₂), low CO₂ (L-CO₂), and very low CO₂ (VL-CO₂). Our transcriptome comparison identified a massive impact of *CIA5* and CO₂ on the transcriptome and revealed an array of gene clusters with distinctive expression patterns that provide insight into the regulatory interaction between *CIA5* and CO₂. Individual gene clusters responded primarily to *CIA5*, to CO₂, or to an interaction between the two. This study of transcriptome-wide gene expression patterns provides insight into the massive impact of these two factors and their interaction on *C. reinhardtii* gene expression in addition to identifying compelling new candidates for CCM functional components.

RESULTS

Identification of Differentially Expressed Genes

This transcriptome study was designed employing three CO₂ acclimation states, H-CO₂ (5% CO₂), L-CO₂ (0.033 to 0.041%), and VL-CO₂ (0.011 to 0.015%), and two strains (genotypes): the *cia5* mutant and its original wild-type progenitor, 137c. Processing of RNA samples on the Illumina Genome Analyzer system yielded more than 12 million reads mapped to the transcriptome for each sample, and more than 90% of these were uniquely mapped to the *C. reinhardtii* genome (see Supplemental Table 1 online). We detected expression for 15,649 of 15,818 filtered Augustus 5.0 gene models (>99% coverage). Since Augustus 5.0 predictions were based on the *Chlamydomonas* Version 4 genome assembly, we also acquired annotation information from the filtered Version 4 model set available from the Joint Genome Initiative database as user annotation references and sources for the common gene names.

As an aid to examining gene expression level distributions, we calculated the reads per kilobase of exon model per million of aligned reads (RPKM) values as normalized expression estimates for each gene model in each sample. The shape of distributions for the average RPKM values are very similar among the six conditions, as are the 5th, 50th, and 95th percentiles of these distributions (see Supplemental Figure 1 online). Also, the calculated correlation coefficients, based on the log-transformed RPKM values after eliminating genes with zero count in either of the two replicates, between the two biological replicates for each condition range from 0.935 to 0.983, indicating high correlation between replicates.

To evaluate the reliability of our RNA-Seq results, we performed quantitative PCR (qPCR) on eight previously studied genes (*CAH1*, *CAH3*, *CAH6*, *CIA5/CCM1*, *HLA3*, *LCIB*, *LCIE*, and *RHP1*) using the same RNA samples as those used for RNA-Seq. These genes were selected to represent a wide range of expression levels and expression patterns under the conditions used. For all eight genes, the expression patterns from RNA-Seq and qPCR agree very well visually and also are highly correlated, with correlation coefficients ranging from 0.92 to 0.995 (see Supplemental Figure 2 online).

After validating our RNA-Seq results with qPCR, we applied a generalized linear model analysis based on a negative binomial distribution and conducted an overall test to determine which genes vary in expression among any of the six treatment groups, where a treatment group is defined by a strain-by-induction condition combination (see Methods for details). While controlling the false discovery rate (FDR) at 2.5% using Benjamini and Hochberg's method (Benjamini and Hochberg 1995), we identified 3678 genes as differentially expressed (DE) among the six treatment groups (see Supplemental Data Set 1 online). This number is similar in scale to the 5884 DE genes at 30, 60, or 180 min after CO₂ deprivation in wild-type *C. reinhardtii* cells reported in the companion publication (Brueggeman et al., 2012).

The overall test identified genes with differential expression in any of the six treatment groups. The transcript levels of these genes might be affected by: (1) the CO₂ concentration, (2) the presence/absence of functional *CIA5*, and/or (3) the interaction of CO₂ concentration and the presence/absence of functional *CIA5*. To provide more detailed information about how the CO₂ level or the presence/absence of *CIA5* affects gene expression, we used a C/S impact model. Under this model, we separately tested for a CO₂ effect (due to varied CO₂ levels; C-effect), a strain effect (due to varied genotypes; S-effect), and an interaction effect between CO₂ levels and genotype (CS-effect) using the generalized linear model (C/S impact test) as described in Methods. When we control the FDR level at 2.5%, this C/S impact test identifies most of the DE genes, with only 165 of the 3678 DE genes identified from the overall test failing to show significance for any one of the three possible effects. Among the other 3513 genes, 2230 exhibit significant C-effect, 2787 exhibit significant S-effect, and 372 exhibit significant CS-effect (see Supplemental Data Set 1 online).

To facilitate a closer comparison of previously reported LCI genes with our results, we also conducted a pairwise comparison of our expression data for the wild type in H-CO₂, L-CO₂, and VL-CO₂ conditions using the *DESeq* package (Anders and Huber, 2010), which was reported to be one of the best methods for identifying DE genes between two treatment groups (Kvam et al., 2012). When we controlled FDR at level 2.5% using Benjamini and Hochberg's method (Benjamini and Hochberg, 1995), we identified 345 genes DE for the L-CO₂ versus H-CO₂ pairwise comparison and 696 genes DE for the VL-CO₂ versus H-CO₂ pairwise comparison (see Supplemental Data Set 2 online). Surprisingly, no genes were identified as DE for the VL-CO₂ versus L-CO₂ pairwise comparison.

Reproducibility across Laboratories

The companion study by Brueggeman et al. (2012) focused exclusively on the effects of CO₂ deprivation on gene expression. Their focus on the time course for induction from 0 to 3 h nicely complements our study, which compares the impact of CO₂ deprivation and *CIA5* on gene expression following a 4-h induction in limiting CO₂. Their findings support many of our observations and conclusions regarding transcriptome changes associated with CO₂ deprivation. Nonetheless, the two studies were conducted completely independently and involved significant differences in experimental conditions (e.g., light and

temperature) and in the *C. reinhardtii* strains used. Therefore, the differences found in the patterns and the magnitude of gene expression between these two studies are not unexpected (i.e., considerably lower interlaboratory reproducibility than intra-laboratory reproducibility is expected). Further details about the reproducibility of our expression estimates and their correlation with results from our companion article can be found at the end of Methods and in Supplemental Figures 3 to 5 online.

Clusters of Genes with Similar Expression Patterns

We applied a model-based clustering algorithm to identify distinct gene expression profiles among identified DE genes and chose a total of 16 clusters to maintain as few tight clusters as possible while including most of the distinct expression patterns (Figure 1). Each gray line in Figure 1 represents the expression pattern for an individual gene, and the single black line indicates the average behavior for all genes in that cluster.

When sorted by cluster, the C/S impact test results (see Supplemental Figure 6 online) confirmed many of the visually observed patterns in the clusters. For example, gene expression patterns in clusters 1, 2, 3, 10, 11, and 13, the CIA5 clusters, appear to be affected mainly by the presence/absence of CIA5 but only minimally by CO₂. In agreement with this, 1060 (~76%) of the 1396 genes in these six CIA5 clusters exhibit only a significant S-effect (no C-effect or CS-effect).

By contrast, the expression patterns in clusters 4, 7, and 9, the CO₂ clusters, appear to respond to variation in CO₂, with little apparent difference between the genotypes. Accordingly, 415 of the 764 genes in these three CO₂ clusters exhibit only a significant C-effect (no S-effect or CS-effect). Like those in the CO₂ clusters, genes in clusters 6 and 12 also exhibit visually parallel changes in response to changing CO₂ between the genotypes but also show a slightly larger expression shift between the genotypes (Figure 1). Many genes in these two pseudo-CO₂ clusters exhibit C+S effects or only C-effect, but the larger proportion of genes exhibiting S-effect distinguishes them from the CO₂ clusters (see Supplemental Figure 6 online).

Clusters 8, 14, and 15, the CCM clusters, exhibit a pattern of induction or upregulation under limiting CO₂ and repression by the absence of CIA5. These three CCM clusters also contain a considerable number of genes exhibiting significant C+S-effects (both C- and S-effects) and C+S+CS-effects (all C-, S-, and CS-effects) as well as a large number of genes exhibiting only S-effects and few or no genes exhibiting only C-effects (see Supplemental Figure 6 online).

Genes in clusters 5 and 16 show the mildest changes over the six strain-by-treatment combinations (see Supplemental Figure 6 online) and exhibit a mix of genes with all three effects (C-effect, S-effect, and CS-effect). These two clusters also include the largest proportion of genes that were detected by the overall test but not the individual test for any one of the three possible effects from the C/S impact model.

Functional Implications of the Gene Expression Clusters

In addition to the distribution of genes into clusters based on similar expression patterns, we used two complementary methods

to examine the DE genes within each cluster for commonalities of function: the Algal Functional Annotation Tool (Lopez et al., 2011) and manual curation. In employing the Algal Functional Annotation Tool, we used the Gene Ontology (GO) terms based on orthology to *Arabidopsis thaliana* to overcome the limitation of available annotations for *C. reinhardtii*. We compiled all GO terms that showed statistical significance ($P < 0.01$) in at least one gene cluster and generated a summary heat map to visualize an overview of the resulting functional information by clusters (see Supplemental Figure 7 online). A detailed list of GO terms identified for the clusters can be found in Supplemental Data Set 3 online. In the heat map, GO terms were subjected to hierarchical clustering so that gene clusters with common significant ontology terms are placed close to each other in the tree. Although details of the identified GO terms and associated genes corresponding to the heat map are found in Supplemental Data Set 3 online, Supplemental Figure 7 online illustrates that very few of the significant GO terms (20 out of 210) overlap among any of the 16 cluster entries, which suggests that the genes separated into clusters based on distinctive expression patterns also tend to be involved in varied biological processes, providing independent support for our clustering results.

In addition to tabulating the significant GO terms associated with each gene cluster, the total number of unique genes represented within all of the significant GO categories for each cluster was determined. For example, Table 1 indicates that 22 GO terms were identified by the Algal Functional Annotation Tool to be associated with cluster 1, but these 22 GO terms represent only three unique genes, since each of the three genes is associated with multiple GO terms. This example is not unique; in many of the clusters, the significant GO category hits represented only a small number of individual genes, even if the number of GO category hits was high. On the other hand, 60 unique genes (32.1% of the genes) in cluster 5 were included among the significant GO term hits. However, only in six of the clusters, (4, 5, 6, 9, 10, and 11) were at least 8% of the genes in the cluster identified among the GO hits.

Because of the relative paucity of functional annotation in the *C. reinhardtii* genome, the Algal Functional Annotation Tool was unable to provide much functional information for more than a few gene clusters. Therefore, we also employed manual curation to place DE genes into eight broad functional categories (see Supplemental Data Set 4 online). Not surprisingly, the most abundant manual functional category of DE genes in all 16 clusters was “unknown,” which is represented by the difference between 100% and the sum of all other functional categories for each cluster in Figure 2 and accounts for 38 to 62% of the genes in each. Among the 16 clusters, the most abundant of the eight manual categories after “unknown,” are “metabolism,” “signaling,” and “gene expression and regulation.” The relative distribution of DE genes among these eight manually curated categories is illustrated for each gene cluster in Figure 2, and a compilation of the primary functional category in each cluster identified as including the largest proportion of genes (excluding the “unknown” category) is summarized in Table 1.

No single functional category among the genes in each major cluster group (CIA5, CO₂, and CCM clusters) was consistently apparent by either method. However, those CIA5 clusters (1, 3,

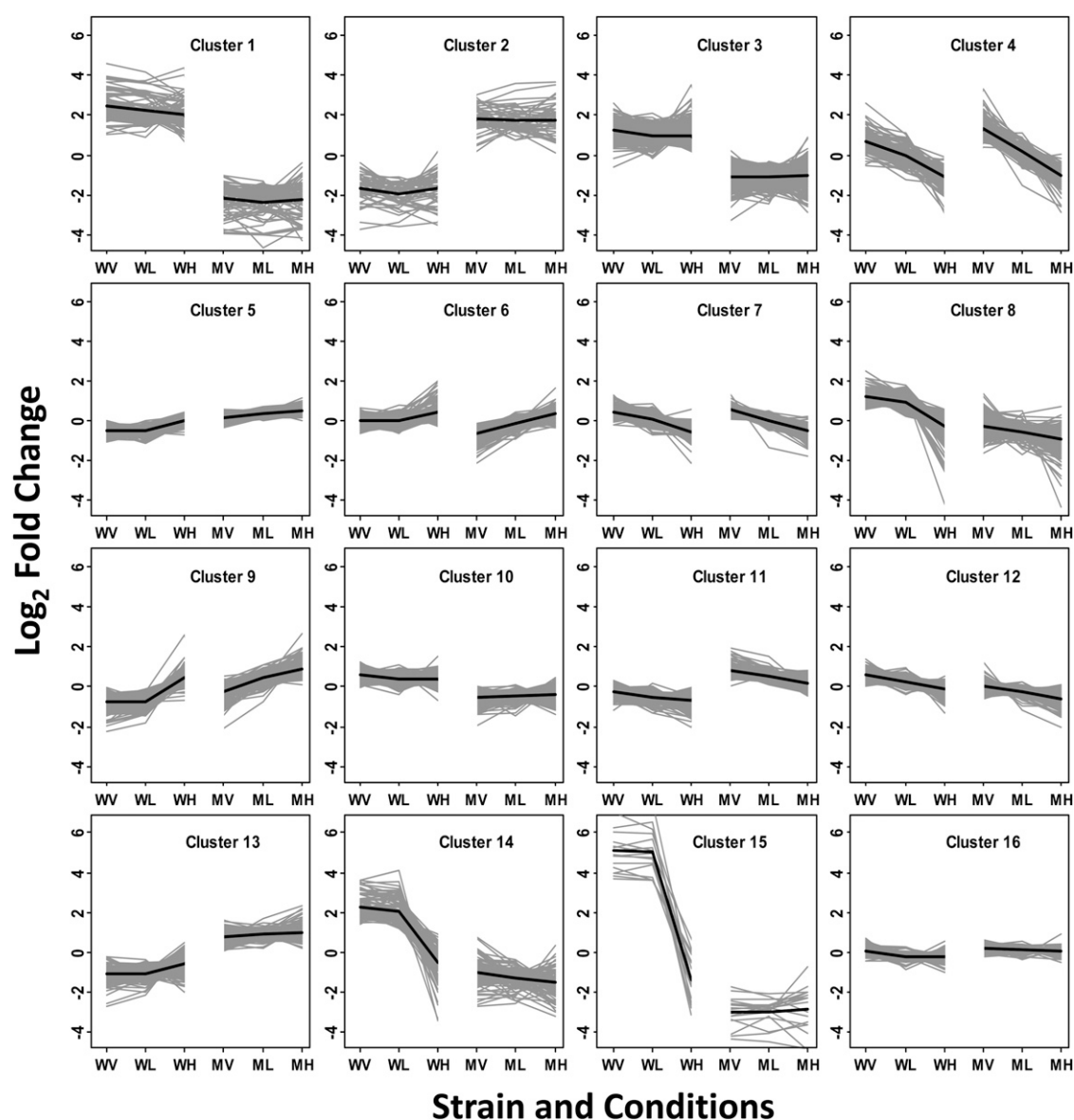


Figure 1. Clustering.

The expression patterns of 3678 selected DE genes for 16 clusters. The horizontal axis indicates each strain and CO₂ induction condition: WV, the wild type under VL-CO₂ induction; WL, the wild type under L-CO₂ induction; WH, the wild type under H-CO₂ induction; MV, *cia5* under VL-CO₂ induction; ML, *cia5* under L-CO₂ induction; MH, *cia5* under H-CO₂ induction. The vertical axis indicates the log₂ fold change calculated between each condition and the average across all six conditions. Each gray line symbolizes the expression pattern of one gene, and the bold back line illustrates the average expression pattern of all genes in each cluster.

and 10) with higher gene expression in the wild type all have signaling as the primary functional category, whereas those clusters (2, 11, and 13) with higher gene expression in *cia5* have metabolism as the primary functional category. Furthermore, the functional categories of signaling and gene expression together accounted for more than half of the genes in CIA5 clusters 1, 3, and 10, excluding the unknown category. Of these CIA5 clusters, only clusters 10 and 11 contained more than 8% of the genes identified as GO category hits, but these GO hits agreed

with the primary functional category of signaling for cluster 10, in that they fell in the general areas of intracellular trafficking, proteolysis, and regulation of processes, and of metabolism for cluster 11, in that they fell in the general area of metabolic processes (see Supplemental Data Set 3 online).

Similarly, the CO₂ cluster 9 with increased transcript abundance at higher CO₂ concentrations has gene expression as the primary functional category, whereas those clusters (4 and 7) with increased gene expression at lower CO₂ concentration

Table 1. GO Categories of Clusters

Clusters			Functional Annotation Tool				Manual Curation	
Cluster	Total Genes	Cluster Group	GO Terms	Unique Genes	Unique Genes (%)	Main GO Terms ^a	Primary Functional Category	Total (%)
1	124	CIA5	22	3	2.4%	N/S	Signaling	16%
2	95	CIA5	9	4	4.2%	N/S	Metabolism	19%
3	387	CIA5	25	8	2.1%	N/S	Signaling	14%
4	150	CO ₂	45	15	10.0%	Catabolic processes	Metabolism	24%
5	187	–	33	60	32.1%	Biosynthetic processes	Metabolism	29%
6	240	–	10	30	12.5%	RNA modification; protein localization	Gene expression regulation	23%
7	243	CO ₂	4	7	2.9%	N/S	Metabolism	16%
8	360	CCM	6	8	2.2%	N/S	Metabolism	12%
9	371	CO ₂	23	49	13.2%	RNA processes, nitrogen metabolism	Gene expression regulation	28%
10	460	CIA5	34	63	13.7%	Intracellular trafficking, proteolysis, regulation of processes	Signaling	19%
11	183	CIA5	10	15	8.2%	Small molecule metabolic processes	Metabolism	22%
12	463	–	1	3	0.7%	N/S	Signaling	13%
13	147	CIA5	2	3	2.0%	N/S	Metabolism	32%
14	138	CCM	6	3	2.2%	N/S	Signaling	14%
15	35	CCM	3	1	2.9%	N/S	Metabolism	20%
16	95	–	1	3	3.2%	N/S	Metabolism	20%

Summary of the identified GO terms and primary functional categories within the 16 clusters using the Algal Functional Annotation tool and manual curation, respectively.

^aN/S indicates that significant GO term hits included less than 5% of the unique genes in the cluster.

have metabolism as the primary functional category. Furthermore, the functional categories of gene expression and signaling combined accounted for more than half of the genes in CO₂ cluster 9, excluding the unknown category. Of the three CO₂ clusters, only 4 and 9 each contained more than 8% of the genes identified as GO category hits, and in both cases, these GO hits agreed with the primary functional category identified. In CO₂ cluster 9, which had gene expression as its primary functional category, the GO category hits fell in the general areas of RNA processes and nitrogen metabolism (see Supplemental Data Set 3 online). For CO₂ cluster 4, which had metabolism identified as its primary functional category, the GO category hits fell in the general area of catabolic processes (see Supplemental Data Set 3 online), and a large proportion of the cluster 4 genes in the manually curated metabolism category were putative catabolic genes (see Supplemental Data Set 4 online).

Among the CCM clusters, the various functional categories appeared to be relatively evenly dispersed, with the exception of cluster 15. Although cluster 15 had the somewhat common category of metabolism as its primary functional category, it is notable in having, among all the clusters, the highest proportion (~14%) of manually curated genes in the transport functional category.

Key CO₂ Assimilation-Related Genes and Pathways

In addition to the segregation of genes into broad functional categories, we also analyzed the distribution of specific groups of genes among the gene expression pattern clusters, such as previously reported LCI genes, Calvin cycle genes, photorespiratory pathway genes, and CA genes.

Of 2274 genes exhibiting a C-effect and/or a CS-effect (see Supplemental Data Set 1 online), and thus indicating a statistically significant response to CO₂ concentration, 1350 were upregulated in wild-type L-CO₂ versus H-CO₂, and 418 had a fold change of 2 or greater. This selection of genes is the most comparable to

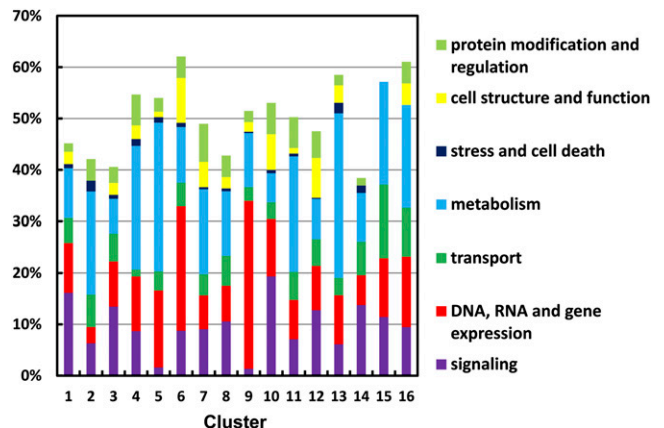


Figure 2. Distribution of Genes in Manual Functional Categories within Each Cluster.

The functional categories (protein modification and regulation, cell structure and function, stress and cell death, metabolism, transport, gene expression and regulation, and signaling) were determined manually based on a combination of existing annotation and automated identification of functional domains. Percentages indicate the sum of genes in each functional category (indicated by color). The difference between the summed percentage and 100% represents the “unknown” category, which is not included.

classic LCI genes reported previously (Chen et al., 1996; Somanchi and Moroney, 1999; Miura et al., 2004; Wang et al., 2005; Wang and Spalding, 2006; Yamano and Fukuzawa, 2009). We selected 106 of these previously reported LCI genes for a direct comparison with genes identified as having a C-effect or CS-effect. Among these 106 previously reported LCI genes, 49 exhibit a C-effect or CS-effect, and 45 of these were upregulated in either L-CO₂ or VL-CO₂ conditions compared with H-CO₂ in the wild-type strain (see Supplemental Data Set 5 online). We also used a recently proposed statistical method implemented in the *Bioconductor* package *DESeq* (Anders and Huber, 2010) to perform a direct, pairwise comparison of gene expression for H-CO₂ versus either L-CO₂ or VL-CO₂, which identified a highly overlapping but slightly different list of 40 previously reported LCI genes as upregulated in our experiment. In combination with the C/S impact model, the *DESeq* analysis supports 53 of the previously reported LCI genes as upregulated in either L-CO₂ or VL-CO₂ (see Supplemental Data Set 5 online).

Data included in our companion article (Brueggeman et al., 2012) demonstrate a low-CO₂ upregulation of 40 of the 106 previously identified LCI genes, and 35 of these overlap with the 53 genes identified here as being upregulated by L-CO₂ or VL-CO₂. In combination, our data and the data from Brueggeman et al. (2012) provide support for upregulation of 60 of the 106 previously reported LCI genes. In addition to showing downregulation for three of the same four previously reported LCI genes that our data identify as downregulated, our companion article identifies an additional two previously reported LCI genes that exhibit downregulation under their experimental conditions (see Supplemental Data Set 5 online).

From our list of 49 previously reported LCI genes showing a C-effect or CS-effect, 36 genes fall into the CCM clusters (8, 14, and 15), and an additional seven genes in the CCM clusters were identified as upregulated in L-CO₂ or VL-CO₂ based on the pairwise *DESeq* analysis (see Supplemental Data Set 5 online). To explore this relationship further, we selected 10 intensively studied, CIA5-regulated, LCI genes (*CAH1*, *CAH3*, *CCP1*, *CCP2*, *HLA3*, *LCIA*, *LCIB*, *LCIC*, *LCI1*, and *LRI1*; highlighted in Supplemental Data Set 5 online) implicated as functionally involved in the CCM (Spalding, 2008; Wang et al., 2011) and found all to be contained in CCM clusters 8, 14, and 15, and all except *CAH3* were identified as DE by our companion article (Brueggeman et al., 2012). Figure 3 provides a schematic model of the proposed *C. reinhardtii* CCM, including C_i uptake and accumulation processes (modified from Wang et al., 2011), including identified and proposed locations of the various CAs (Moroney et al., 2011). A major proportion of the CCM/CA genes in this model were included in CCM clusters 15, 14, or 8, providing additional validation of our clustering results.

Although a large proportion of the previously reported LCI genes identified here as DE genes were found to be associated with CCM clusters 8, 14, and 15, a substantial number also were associated with CO₂ clusters 7 and 9. Of the 53 previously reported LCI genes supported by our data, seven fell into CO₂ cluster 7, four genes fell into CO₂ cluster 9, and one each into CIA5 clusters 11 and 12 (see Supplemental Data Set 5 online). Six previously reported LCI genes that were not supported as LCI genes by our data (i.e., no C-effect or CS-effect and not DE

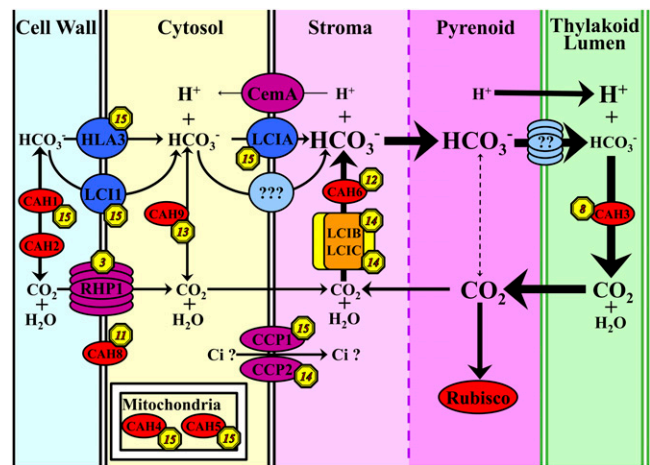


Figure 3. Gene Cluster Distribution within a Hypothetical CCM/C_i Transport Model.

The cluster label for each gene is indicated by a yellow octagon containing a cluster number. In this schematic representation of the CCM, most of the putative CCM elements and many previously identified CO₂-responsive genes, including the putative C_i transporters *HLA3*, *LCI1*, *LCIA*, *CCP1*, and *CCP2* and CCM-related CAs *CAH1* and *CAH3*, and other identified CCM genes like *LCIB* and *LCIC* are indicated as having expression patterns categorized in the “CCM clusters (clusters 8, 14, and 15).” This figure is modified from Wang et al. (2011), with the addition of the LCI chloroplast membrane proteins *CCP1* and *CCP2* (Chen et al., 1997) and CA locations (Moroney et al., 2011). Transport proteins with demonstrated CCM function are shown in dark blue, known transport proteins with suspected CCM function are shown in purple, predicted but unknown transport proteins are shown in light blue, known soluble enzymes are shown in red, and the soluble *LCIB/LCIC* complex is shown in orange and yellow.

based on the *DESeq* analysis) were identified as DE genes but fell mostly into CIA5 clusters 3, 10, 11, and 13.

By visual inspection, the gene expression pattern in CCM cluster 15 shows very low expression in H-CO₂ and induction in VL-CO₂ and L-CO₂ conditions for the wild type and very low expression in any CO₂ conditions for the *cia5* mutant. CCM clusters 8 and 14, on the other hand, show only upregulation of expression under VL-CO₂ and L-CO₂ conditions for the wild type, relative to the modest expression in H-CO₂ conditions, and almost equally low expression under any CO₂ conditions for the *cia5* mutant. Thus, the patterns for CCM clusters 8, 14, and 15 progress from mild upregulation of expression to high-level induction, respectively. Only 35 genes showed the high-level induction and were grouped in CCM cluster 15, so every gene in this cluster is listed in Table 2, and all genes in clusters 8, 14, and 15 are listed in Supplemental Data Set 6 online.

Based on our manual functional curation, CCM cluster 15 contains a relatively large proportion of genes in the manually annotated transport functional category (Figure 2) and includes essentially all the genes for which there is either compelling evidence for a C_i transport role for the gene product in the CCM (*LCIA*, *LCI1*, and *HLA3*) or a strong argument for the gene product as a good candidate for C_i transport (*CCP1*). As with all

Table 2. Genes in Cluster 15

Name	Protein ID ^a	Description ^b	Average RPKM ^c	Significant Effects ^d	Primary Functional Category ^e
<i>CAH1</i>	522126	CA, periplasmic, α type	1223.8	C+S+CS	Metabolism
<i>CAH4</i>	522732	Mitochondrial CA, β type	226.5	C+S+CS	Metabolism
<i>CAH5</i>	522733	Mitochondrial CA, β type	157.3	C+S+CS	Metabolism
<i>CCP1</i>	522130	LCI chloroplast envelope protein	162.0	C+S+CS	Transport
<i>CGL28</i>	510019	RNA binding protein	200.7	C+S+CS	Unknown
<i>CYC6</i>	516039	Cytochrome c6	1.2	S	Metabolism
<i>DNJ15</i>	514023	DnaJ-like protein	12.8	S	Gene Expression
<i>DNJ31</i>	518238	DnaJ-like protein	13.1	S	Gene Expression
<i>*HFO7</i>	523344	Histone H4	<0.1	–	Gene Expression
<i>HLA3</i>	518934	ATP binding cassette transporter	289.5	C+S	Transport
<i>*KIR1</i>	526069	Keto acid isomerase-like protein	<0.1	–	Unknown
<i>LCI1</i>	520703	LCI membrane protein	224.0	C+S	Transport
<i>LCI23</i>	523507	LCI protein	75.8	C+S	Unknown (TM)
<i>LCIE</i>	522129	LCIB-like gene	1.6	S	Metabolism
<i>LCR1</i>	519760	Low-CO ₂ response regulator	79.0	C+S	Gene Expression
<i>LHCSR2</i>	525378	Stress-related chlorophyll a/b binding protein 2	45.7	C+S+CS	Metabolism
<i>LHCSR3</i>	525376	Stress-related chlorophyll a/b binding protein 3	51.7	C+S+CS	Metabolism
<i>NAR1.2</i>	524076	Anion transporter; LCIA	209.7	C+S	Transport
–	516770	PRLI-interacting factor L	44.9	S	Signaling
–	509757	Acetyltransferase	27.5	C+S	Unknown
–	519249	Ser/Thr protein kinase	53.5	S	Signaling
–	522781	ND	4.85	S	Unknown (TM)
–	516290	ND	51.5	C+S	Transport
–	510680	ND	44.6	C+S	Unknown (TM)
–	520458	ND	20.7	S+CS	Unknown
–	512353	ND	16.8	C+S+CS	Unknown (TM)
–	522486	ND	8.7	C+S	Signaling
–	524386	ND	6.4	S	Unknown (TM)
–	524387	ND	2.3	S	Unknown
*–	512735	ND	<0.1	S	Unknown
*–	519540	ND	<0.1	–	Unknown
*–	522103	ND	<0.1	–	Unknown
*–	510710	ND	<0.1	–	Signaling
*–	518019	ND	<0.1	–	Unknown
*–	511100	ND	<0.1	–	Unknown

Asterisks indicate genes with an average expression level lower than 0.05 RPKM and “–” indicates unnamed gene.

^aAugustus 5.0 gene model protein ID.

^bND means no description available.

^cAverage RPKM across all six treatment conditions.

^dIndividual effect having a q-value <0.025 by C/S impact test, where “C” means CO₂ effect, “S” means strain effect, “CS” means interaction effect, and “–” means no significant C/S impact effect.

^eResult from our manual curation, where “unknown (TM)” indicates gene of unknown function containing at least one putative transmembrane domain.

the clusters, a large proportion (15/35) of the genes in CCM cluster 15 falls into the “unknown” functional category. However, it is notable that five of the 15 genes of unknown function in cluster 15 are putative transmembrane proteins.

Within CCM cluster 15, all 17 genes with significant C-effects also exhibit S-effects (includes *CAH1*, *CAH4*, *CAH5*, *LCI1*, *LCR1*, *CCP1*, *HLA3*, and *LCIA*), and eight of these (includes *CAH1*, *CAH4*, *CAH5*, and *CCP1*) also have a significant CS-effect. Seven genes that did not exhibit any significant C/S impact effects have expression levels in the lowest 3% of genes, with a mean RPKM lower than 0.023 for all seven genes. Of the remaining 11 genes in CCM cluster 15 with significant expression levels, all exhibit only S-effect except one (protein ID 520458; also shows CS-effect).

CAs catalyze the reversible hydration of CO₂ to HCO₃[–] and serve critical roles for the CCM (Moroney et al., 2011) (Figure 3). Among the nine identified α and β CA genes (Table 3), *CAH1*, *CAH4*, and *CAH5* fell into CCM cluster 15 and have all three significant C+S+CS-effects, as described above. These three CA genes are strongly induced in low CO₂ and thus may be directly involved in the C_i transport and accumulation process of the CCM or at least in the acclimation to low CO₂. *CAH3*, the thylakoid lumen CA required for dehydration of stromal HCO₃ (Moroney et al., 2011), exhibits both significant C+S-effects and was placed in cluster 8, which contains genes whose visual expression patterns indicate modest upregulation in response to limiting CO₂. CA genes *CAH8* and *CAH9* showed mainly S-effects and fell into CIA5 clusters 11 and 13, respectively, and

Table 3. CAs

Name	Protein ID ^a	Description and Subcellular Location	q-Values ^b	Cluster ^c	Significant Effects ^d
CAH1	522126	α -CA, periplasm	3.4E-04	15	C+S+CS
CAH2	522125	α -CA, periplasm	3.2E-01	—	—
CAH3	526413	α -CA, thylakoid lumen	1.5E-02	8	C+S
CAH4	522732	β -CA, mitochondria	2.7E-03	15	C+S+CS
CAH5	522733	β -CA, mitochondria	3.4E-03	15	C+S+CS
CAH6	512520	β -CA, chloroplast stroma	5.4E-03	12	C+S
CAH7	515107	β -CA, unknown	2.5E-02	—	—
CAH8	526207	β -CA, plasma membrane	1.6E-02	11	S
CAH9	522626	β -CA, cytoplasm	2.3E-02	13	S

^aAugustus 5.0 gene model protein ID.^bq-values calculated by overall test.^cA “—” indicates the gene was not identified as DE in overall test.^dIndividual effect having a q-value <0.025 by C/S impact test, where “C” means CO₂ effect, “S” means strain effect, “CS” means interaction effect, and “—” indicates the gene was not identified as DE in overall test so was not included in C/S impact test.

CAH6 showed both C+S-effects and fell into cluster 12. CAH2 and CAH7 were not identified as DE genes.

We also scrutinized the genes encoding enzymes of the Calvin cycle and the photorespiratory pathway (Spalding, 2009), since these important carbon metabolism pathways are expected to respond to CO₂ concentration (Figure 4). Eight of the 15 genes involved in the Calvin cycle were DE in our experiment. Two fructose biphosphate aldolase genes *FBA1* and *FBA3*, the sedoheptulose biphosphatase gene *SEBP1*, and one of the two Rubisco small subunit genes, *RBCS1*, were found in CIA5 clusters 11 and 13, both of which show increased gene expression in the *cia5* mutant but relatively little effect of CO₂ concentration. Two critical kinase-encoding genes, *phosphoglycerate kinase1* (*PGK1*) and *phosphoribulokinase1* (*PRK1*), and the fructose biphosphatase gene *FBP1* were included in cluster 5, which shows a pattern of mildly increasing gene expression with increasing CO₂ concentration as well as mildly increased gene expression in the *cia5* mutant. The *ribose-5-phosphate isomerase1* (*RPI1*) gene was in CO₂ cluster 9, which shows significantly increased expression under higher CO₂ concentration but only modest expression increase in the *cia5* mutant. Thus, aside from *PGK1* and *RPI1*, in which both C-effect and S-effect were detected, all DE genes from the Calvin cycle show only S-effects and increased expression in *cia5*.

On the other hand, the expression of photorespiratory pathway genes was strongly affected by the CO₂ concentration; many of the genes were upregulated in L-CO₂ and VL-CO₂ (Figure 4). Accordingly, the photorespiratory genes *alanine aminotransferase1* (*AAT1*), *glycerate kinase* (*GLYK*), *glycolate dehydrogenase* (*GYP1*), *hydroxypyruvate reductase1* (*HPR1*), and *serine glyoxylate aminotransferase1* (*SGAT1*) and all Gly decarboxylase complex subunit genes, except *glycine cleavage system*, *H-protein* (*GCSH*) and *dihydrolipoyl dehydrogenase1* (*DLDH1*), fell into CCM cluster 8, even though the Algal Functional Annotation Tool only identified two genes, *AAT1* and *HPR1*, among the GO hits for photorespiration in cluster 8 (see Supplemental Data Set 3 online). These cluster 8 photorespiratory genes, which encode enzymes spanning the entire pathway from glycolate to phosphoglycerate, appear to be

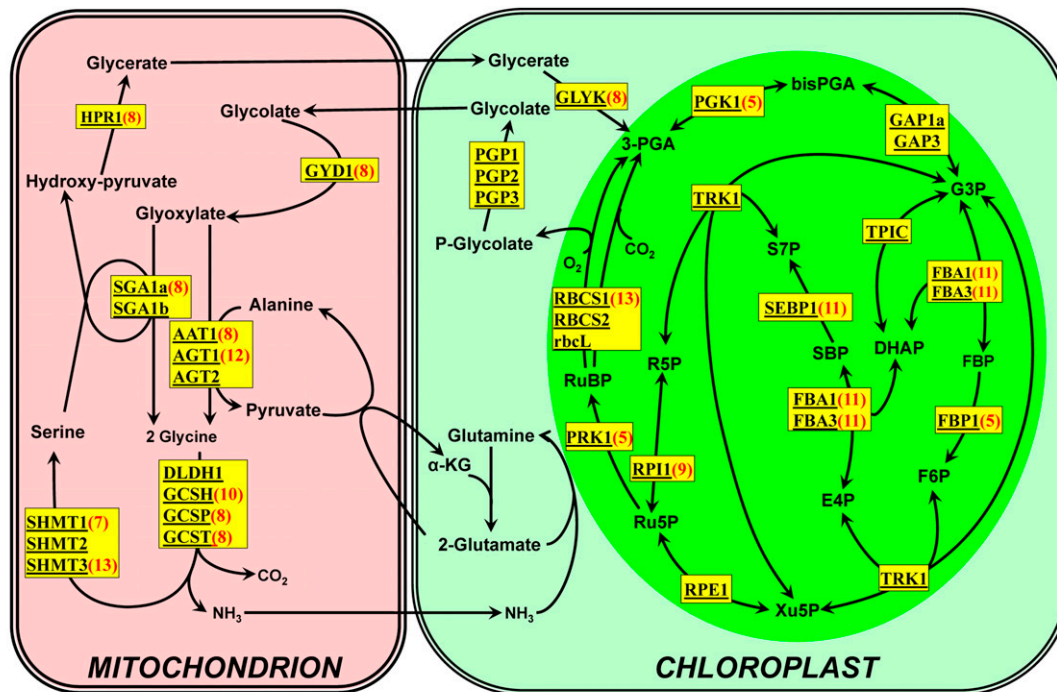
regulated by both CIA5 and CO₂; accordingly, all exhibited C-effects and S-effects, and all, except *AAT1* and *HPR1*, exhibited CS-effects.

Of those photorespiratory pathway genes not in CCM cluster 8, *GCSH* and *serine hydroxymethyltransferase3* (*SHMT3*) were found in CIA5 clusters 10 and 13, respectively, with S-effects only, *SHMT1* was captured in CO₂ cluster 7 with only significant C-effect, and *alanine-glyoxylate transaminase1* (*AGT1*) was found in cluster 12 with a significant C+S-effect. Some photorespiratory genes, such as the three phosphoglycolate phosphatase genes *PGP1*, *PGP2*, and *PGP3*, were not identified as being DE in our experiment even though phosphoglycolate phosphatase activity was reported to increase in response to limiting CO₂ (Marek and Spalding, 1991; Tural and Moroney, 2005). One isoform of Ala-glyoxylate transaminase (*AGT2*), one isoform of Ser hydroxymethyltransferase (*SHMT2*), and the Gly decarboxylase complex subunit *DLDH1* also were not identified as DE genes under the conditions used.

DISCUSSION

Identification of DE Genes

In this article, our primary objective was to gain insight into the transcriptome-wide changes in the patterns of gene expression that occur in response to the interaction between CO₂ concentration and the transcription regulator CIA5. An additional benefit expected was the identification of candidate genes that may play significant roles in the CCM. To address these objectives, we analyzed the gene expression profiles of two genotypes, the wild type (137c) and *cia5*, under three different CO₂ concentrations using an overall test to identify 3678 genes that showed differential expression in at least one of the six treatments (two genotypes \times three conditions). This identification of over 3600 DE genes, which represents almost 20% of the *C. reinhardtii* transcriptome, revealed massive changes in gene expression in response to the combination of CO₂ concentration changes and the presence/absence of CIA5.



Calvin Cycle				Photorespiration			
Name	Description	C	S.E.	Name	Description	C	S.E.
FBA1	Fructose-1,6-bisphosphate aldolase	11	S	AAT1	Alanine aminotransferase	8	S
FBA3	Fructose-1,6-bisphosphate aldolase	11	S	AGT1	Alanine-glyoxylate transaminase	12	C+S
FBP1	Fructose-1,6-bisphosphatase	5	S	AGT2	Alanine-glyoxylate transaminase	-	-
GAP1.a	Glyceraldehyde 3-phosphate dehydrogenase	-	-	DLDH1	Dihydrolipoyl dehydrogenase	-	-
GAP3	Glyceraldehyde-3-Phosphate dehydrogenase	-	-	GCSH	Glycine cleavage system, H-protein	10	S
PGK1	Phosphoglycerate kinase	5	C+S	GCSP	Glycine cleavage system, P protein	8	C+S+CS
PRK1	Phosphoribulokinase	5	S	GCST	Glycine cleavage system, T protein	8	C+S+CS
RBCS1	Rubisco small subunit 1	13	S	GLYK	Glycerate kinase	8	C+S+CS
RBCS2A	Rubisco small subunit 2	-	-	GYD1	Glycolate dehydrogenase	8	C+S+CS
RPE1	Ribulose phosphate-3-epimerase	-	-	HPRI	Hydroxypyruvate reductase	8	C+S
RPI1	Ribose-5-phosphate isomerase	9	C+S	PGP1	Phosphoglycolate phosphatase 1	-	-
SEBP1	Sedoheptulose-1,7-bisphosphatase	11	S	PGP2	Phosphoglycolate phosphatase	-	-
TAL2	Transaldolase	-	-	PGP3	Phosphoglycolate phosphatase	-	-
TPIC	Triose phosphate isomerase	-	-	SGA1.a	Serine glyoxylate aminotransferase	8	C+S+CS
TRK1	Transketolase	-	-	SHMT1	Serine hydroxymethyltransferase	7	C
				SHMT2	Serine hydroxymethyltransferase 2	-	-
				SHMT3	Serine hydroxymethyltransferase 3	13	S

Figure 4. Genes Involved in the Calvin Cycle and Photorespiration.

(A) Schematic of the Calvin cycle and photorespiration pathway in *C. reinhardtii* (Spalding, 2009). Yellow boxes indicate genes involved in each reaction, and the red numbers in parentheses indicate the cluster in which each gene was found.

(B) Summary of detailed information about each gene. C, cluster number (a “-” indicates the gene was not identified as DE in overall test and not assigned a cluster); S.E., significant effects, which are individual effects having a q-value <0.025 by the C/S impact test, where C is CO₂ effect, S is strain effect, CS is CO₂ and strain interaction effect, and “-” indicates the gene was not identified as DE in overall test so was not included in C/S impact test.

Further detailed analysis of the 3678 DE genes was performed using two additional methods: (1) C/S impact tests for C-effects, S-effects, and CS-effects, for each gene; and (2) a cluster analysis of the gene expression patterns across the six conditions. Whereas cluster analysis grouped DE genes with similar expression patterns, the C/S impact test provided quantitative evaluations of individual environmental induction and strain effects. The majority of genes identified as DE genes by the overall test showed one or more significant C/S impact effects when tested for C-, S-, and CS-effects. Only ~5% (165 out of 3678) of the DE genes identified by the overall test were not identified as having significant individual effects in the C/S impact test, possibly due to different power of detection inherent in the overall test and the C/S impact test.

Cluster analysis, in combination with identification of individual C-effects, S-effects, and CS-effects, revealed clusters of genes regulated primarily by CIA5 (predominantly S-effects; CIA5 clusters), regulated primarily by CO₂ (predominantly C-effects; CO₂ clusters), and regulated by interaction of CO₂ and CIA5 (predominately CS-effects and combinations of C-effects, S-effects, and CS-effects). The delineation of these clusters directly addressed our overall objective of gaining insight into the patterns of gene expression in response to interaction between CO₂ and CIA5, as well as revealing specific genes regulated by CO₂, by CIA5, and by the interaction of CO₂ and CIA5. Based on reports of induction or upregulation of CCM-related genes in low CO₂, genes functionally involved in the *C. reinhardtii* CCM were expected to be among the third general group of genes, those regulated by both CO₂ and CIA5.

Comparison with Previously Reported LCI Genes

Although our major objective was to discover a spectrum of gene expression patterns in response to the interaction between CO₂ and CIA5, we also performed direct pairwise comparisons in the wild-type strain between H-CO₂ and either L-CO₂ or VL-CO₂ to provide a more detailed analysis of the differential expression of genes in response to low or limiting CO₂. Because of the historical connection between low-CO₂ upregulated genes and the CCM, we included these DESeq analyses to enrich the comparisons between previously reported LCI genes and DE genes identified in this study.

Because of the interest in the CCM specifically, at least 106 genes have been reported as LCI genes, many of which also reportedly require CIA5 for differential expression (Chen et al., 1996; Somanchi and Moroney, 1999; Miura et al., 2004; Wang et al., 2005; Wang and Spalding, 2006; Yamano and Fukuzawa, 2009). Some of these LCI genes, such as *CAH3*, *LCI1*, *LCIA*, *LCIB*, and *HLA3*, reportedly play important roles in the *C. reinhardtii* CCM (Galván et al., 2002; Wang and Spalding, 2006; Duanmu et al., 2009a, 2009b; Ohnishi et al., 2010), and the function of others, such as *CCP1*, *CCP2*, and *LCIC*, in the CCM also has been implicated (Pollock et al., 2004; Wang and Spalding, 2006; Yamano et al., 2010). However, only 53 of 106 previously reported LCI genes were supported as L-CO₂ or VL-CO₂ upregulated DE genes in this study. This discrepancy is not unexpected because the different strains and different light, CO₂ concentration, and other environmental conditions used among

the various studies almost certainly will result in variations in the genes responding and because DE gene identification may be impacted by a shifting in the population distribution among the cell division cycle phases in response to a shift from H-CO₂ to L-CO₂ conditions (Dillard et al., 2011). In addition, the 4-h induction time used here may not identify genes that are DE only earlier or later than 4 h. Indeed, the companion article by Brueggeman et al. (2012) documents significant changes in gene expression during a 3-h time course following CO₂ depletion but also reports the lack of induction of several previously reported LCI genes. Only 40 previously reported LCI genes were supported by Brueggeman et al. (2012) as low-CO₂ upregulated. In combination with those supported by our data, 60 previously reported LCI genes are supported as upregulated under the conditions used in the two studies combined.

Many previously reported LCI genes have not been further characterized or confirmed beyond initial observations, which in many cases used no statistical procedure to control FDRs (Miura et al., 2004; Yamano and Fukuzawa, 2009). The greater sensitivity of RNA-Seq and our more reliable statistical approach provide significant advantages over previous studies. Therefore, in addition to the impact of environmental and strain differences on the absence of some LCI genes from our list of DE genes, some previously reported LCI genes may not represent bona fide LCI genes. Our data indicate that four previously reported LCI genes are actually downregulated by L-CO₂ or VL-CO₂, and, in addition to supporting the downregulation of three of these four genes, our companion article (Brueggeman et al., 2012) identified two more previously reported LCI genes as downregulated by low CO₂.

The results reported here and in our companion article (Brueggeman et al., 2012) complement and extend past reports of differential expression by supporting 60 previously reported LCI genes, directly contradicting six others, and leaving the remaining 40 as not clearly supported under the conditions used in the two studies. In addition, the two companion studies identified a large number of additional genes as regulated by CO₂, CIA5, or both.

CCM Clusters

Of 57 previously reported LCI genes identified in this study as DE genes, 43 fell into the CCM clusters 8, 14, and 15, all of which exhibited expression patterns expected for classic LCI genes (i.e., high expression for the wild type in L-CO₂ and VL-CO₂ but lower expression in H-CO₂ and consistently lower expression in *cia5* under all CO₂ concentrations). In addition to those in the CCM clusters, 11 of the previously reported LCI genes, including four that were downregulated by low CO₂, fell into CO₂ clusters 7 and 9, which exhibit little impact of the presence/absence of CIA5, suggesting that the genes included are not likely to be involved in the CCM. This illustrates an important value of sorting gene expression patterns into clusters, which provide richer insight into the identification of likely functional CCM genes than provided by the LCI approach alone.

The CCM cluster 15 contains only 35 of the 3678 DE genes but may be a rich source of candidate functional CCM genes. Of the 35 genes in cluster 15, eight have RPKM expression levels lower than 0.05 across all conditions, making them unlikely

candidates for a significant role in the CCM. The remaining 27 genes in CCM cluster 15, which includes all the genes that encode transport proteins strongly implicated or suspected as C_i transporters as well as the CCM regulatory gene *LCR1*, the *LCIB*-like gene *LCIE*, and the well-studied CA genes *CAH1*, *CAH4*, and *CAH5* must be good candidates for a functional or regulatory role in the *C. reinhardtii* CCM. Considering the burden of transporting one of the highest flux inorganic nutrients, as well as the selection against wasting energy on transport when CO_2 is abundant, such an expression pattern is not surprising for genes encoding C_i transporters and other conditionally critical CCM components.

Among the remaining genes of CCM cluster 15, four encoding stress-induced light harvesting chlorophyll proteins, stress-related light harvesting complex protein2 (LHCSR2) and LHCSR3, and DnaJ-like, putative chaperonins, DNJ15 and DNJ31, may represent general stress response elements, and a few genes, such as 522486 (putative guanylate cyclase), 519249 (putative protein kinase), and 516770 (putative PRL1 interacting factor), encode potential signaling elements. However, the most intriguing group of cluster 15 genes may be the six unknown or little known transmembrane protein-encoding genes, including 524386, 512353, 510680, 522781, 516290, and 523507, since their expression patterns parallel those of all likely transporter-encoding genes so far identified. Therefore, these genes rank high as possible undiscovered C_i transporters.

Key CO_2 Assimilation-Related Genes and Pathways outside the CCM

CAs are expected to play important roles in microalgae because of the poor solubility and diffusion rate of CO_2 in water and the critical importance of interconversion of these C_i forms internally. Of the nine confirmed α -CA and β -CA genes (Moroney et al., 2011), seven were identified as DE genes in our experiment (Table 3, Figure 3), which is not unexpected given the importance of C_i uptake and accumulation in the CCM and the well-known differential expression of the three CCM cluster 15 CA genes. S-effect appeared to influence more CA genes than C-effect and CS effect, which reinforces our thoughts about the extent of CIA5 influence. Also, this study confirms CAs as important functional targets for further study regarding the dynamics of the CCM.

The expression of a number of Calvin cycle genes, including one Rubisco small subunit gene, was impacted by the *cia5* mutation. DE genes encoding Calvin cycle enzymes were found in clusters 5, 9, 11, and 13, all of which exhibit increased expression in *cia5* relative to the wild type but which vary in their responses to changes in CO_2 concentration. Reinforcing the implication that the Calvin cycle DE genes respond primarily to CIA5, all these genes exhibited a significant S-effect, with only two, *PGK1* (cluster 5) and *RPI1* (CO_2 cluster 9), exhibiting a significant C-effect. Although we have no clear explanation for a CIA5 role in regulation of several Calvin cycle genes, the increased expression of these genes in the *cia5* mutant argues for a role of CIA5 in carbon assimilation independent of the CO_2 concentration. This observation may reflect a role for CIA5 as a repressor of Calvin cycle genes under as yet unidentified

conditions, where the absence of CIA5 activity might result in a modest increase in expression of these Calvin cycle genes.

Photorespiration results from the low specificity of Rubisco and competes with CO_2 assimilation via the Calvin cycle, so lower CO_2 concentrations increase the Rubisco oxidase reaction relative to the carboxylase reaction and increase the demand for photorespiratory enzymes. The apparent regulation of a number of these genes by CIA5 and CO_2 is consistent with previous reports of low- CO_2 induced expression of photorespiratory pathway genes (Marek and Spalding, 1991; Tural and Moroney, 2005), but, contrary to previous reports, we did not see differential expression of any PGP genes. This discrepancy might be explained if PGP activity is regulated at the post transcriptional level or if the change in PGP gene expression occurs in a time frame not captured by our 4-h induction time point. Unlike the DE Calvin cycle genes, most of the DE photorespiratory pathway genes exhibited significant C-, S-, and CS-effects, rather than just significant S-effects, demonstrating that many of the photorespiratory pathway DE genes are regulated by both CO_2 and CIA5.

Not all photorespiratory genes appear to be regulated by CIA5, but the apparent regulation of a large fraction of them by this protein argues that CIA5 plays a significant role in regulation of the photorespiratory pathway. Notably, those photorespiratory pathway genes that exhibit significant S-effect show a differential expression opposite to that of the Calvin cycle genes (i.e., they have increased expression in the wild type relative to *cia5*). This expression pattern across the genotypes is consistent with CIA5 acting as an inducer of photorespiratory pathway genes in contrast with its putative role as a mild repressor of several Calvin cycle genes.

CIA5 Clusters and the Impact of CIA5

CIA5 appears to serve much broader and more extensive roles than indicated by the phenotype of *cia5*, which grows similar to the wild type either heterotrophically or mixotrophically in acetate or photoautotrophically in H- CO_2 and even grows slowly in L- CO_2 (Spalding, 2008). Most genes in CIA5 clusters 1, 2, 3, 10, 11, and 13 show clear regulation by CIA5 but little regulation by CO_2 concentration, indicating that low- CO_2 activation of CIA5 is not always required for function of CIA5. More than 76% of the 1396 genes in these six clusters exhibit only a significant S-effect (no C-effect or CS-effect), and, including genes that also show a significant C-effect or CS-effect, almost 95% exhibit a significant S-effect. Furthermore, of 3678 identified DE genes, over 62% show a significant S-effect, including those that also exhibit a significant C-effect and/or CS-effect, and more than half of those genes regulated directly or indirectly by CIA5 show only a significant S-effect. Thus, almost 15% of all *C. reinhardtii* genes are regulated in some way by CIA5, and almost 7.5% of all genes are regulated by CIA5 independent of any changes in the CO_2 concentration.

CIA5 is very likely involved in the upstream regulation of multiple physiological processes, and, although its own transcript abundance does not change, the presence/absence of CIA5 (and its potential activation/inactivation) may have a major impact on the expression of genes encoding many secondary

regulatory genes, including those encoding transcription factors and signal transduction components involved in regulation of a number of processes. Consistent with this expectation, manual curation and, in most cases, the Functional Annotation Tool, identified signaling or signaling plus gene expression as key functional categories for the three CIA5 clusters with increased expression in the wild type, arguing that when the presence of CIA5 increases transcript abundance for specific genes, it appears to do so as an upstream activator of positive signaling pathways and/or other gene expression activators. On the other hand, both manual curation and the Functional Annotation Tool pointed to metabolism as the primary functional category for the three CIA5 clusters in which the presence of CIA5 resulted in decreased expression of specific genes (decreased expression in the wild type). Thus, when the presence of CIA5 coincides with the repression of specific genes, CIA5 appears to act as an upstream repressor of specific metabolic functions. Notably, half of the Calvin cycle genes identified as DE fall into these three CIA5 clusters, and most of the others fall in cluster 5, which has somewhat similar characteristics, including decreased gene expression in the wild type and metabolism as primary functional category.

CO₂ Clusters and the Impact of CO₂

Regulation of gene expression by CO₂ concentration also appears to be more extensive than expected. Most genes in the CO₂ clusters 4, 7, and 9 show clear CO₂ concentration regulation but little or no apparent effect of CIA5. Almost 55% of the 764 genes in these three clusters exhibit only a significant C-effect (no S-effect or CS-effect), and, when including those genes that also show a significant S-effect or CS-effect, over 90% exhibit a significant C-effect. Furthermore, of 3678 identified DE genes, over 60% show a significant C-effect, including those that also exhibit a significant S-effect and/or CS-effect, and ~30% of those genes regulated directly or indirectly by CO₂ concentration show only a significant C-effect. Thus, CO₂ concentration significantly affects the expression of over 60% of the DE genes, and more than 14% of all genes detected in this experiment. This means that ~14% of all *C. reinhardtii* genes are regulated by CO₂ concentration, most of which (over 10% of the genes) also exhibit some form of CIA5 regulation. However, almost 4% of all genes are regulated by CO₂ apparently independent of CIA5.

Manual curation and the Functional Annotation Tool both identified gene expression as the key functional category for the CO₂ cluster (cluster 9) with decreased expression of genes in L-CO₂ or VL-CO₂ relative to H-CO₂, which is consistent with either limiting CO₂ acting as an upstream repressor or elevated CO₂ acting as an upstream activator, respectively, of genes involved in regulation of gene expression. On the other hand, manual curation and, in one case, the Functional Annotation Tool, identified metabolism as the primary functional category for the two CO₂ clusters (clusters 4 and 7) with increased expression of genes in L-CO₂ or VL-CO₂ relative to H-CO₂, which is consistent with either limiting CO₂ acting as an upstream activator or elevated CO₂ acting as an upstream repressor, respectively, of genes involved in specific metabolic functions. Notably, both functional characterizations of cluster 4 revealed enrichment in

putative catabolic genes, suggesting that low CO₂ concentrations cause starvation and stimulate the expression of genes involved in degrading and remobilizing existing molecules.

More generally, the abundance of metabolism as a primary functional category in nine of the 16 gene clusters, including CIA5 clusters 2, 11, and 13, CO₂ clusters 4 and 7, and CCM clusters 8 and 15 suggests that a major impact of changes in CO₂ and CIA5 is on the expression of genes encoding metabolic enzymes. This seems reasonable, since large changes in metabolism may well accompany substantial changes in CO₂ concentration. These conjectures also are strongly supported by Brueggeman et al. (2012), who report a marked decrease in expression of numerous genes involved in anabolic processes following CO₂ deprivation. Alternatively, the high frequency of metabolism as a primary functional category also may reflect an annotation bias; metabolism-related genes may be easier to annotate, resulting in their disproportionate representation among the manually annotated genes.

Multiple Acclimation States

Although there is compelling evidence demonstrating a distinction between the VL-CO₂ and L-CO₂ acclimation states of *C. reinhardtii*, none of our transcriptome analyses identified any genes DE between the VL-CO₂ and L-CO₂ induction conditions for the wild type. Since a large number of DE genes were identified for L-CO₂ or VL-CO₂ versus H-CO₂ conditions, the apparent absence of DE genes in the VL-CO₂ versus L-CO₂ comparison likely reflects at least a paucity of DE genes distinguishing these two acclimation states under the conditions used. Based on our data, we suggest at least two possible conclusions regarding the distinction between the L-CO₂ and VL-CO₂ acclimation states: (1) These two acclimation states are controlled at levels beyond transcript abundance, or (2) differential expression of genes distinguishing these two acclimation states is evident only earlier or later than the 4-h acclimation time used in our experiment. On the other hand, if we assume a very limited number of genes are DE in VL-CO₂ versus L-CO₂ under our experimental conditions, our one-time test of >15,000 genes may have elevated the problem of multiple testing and reduced our power of detection. To test this assumption, future experiments could increase the number of biological replicates and/or sequence to a greater depth of coverage.

Summary

This transcriptome study resulted in a number of new insights regarding the global regulation of genes by CO₂ concentration, by CIA5, and by the combination or interaction of CO₂ and CIA5. Gene expression patterns were classified into distinct clusters, many of which could be characterized as responding primarily to CIA5 or CO₂ based on the C/S impact test and visual inspection of the expression patterns. Regulation by CIA5 independent of CO₂ demonstrates that low-CO₂ activation of CIA5 is not essential for its function. Three distinct gene expression clusters with response to both CIA5 and CO₂ were clearly associated with CCM-related genes and may prove to represent a rich source of candidates for new CCM components, especially cluster 15,

which may contain a significant number of putative CCM-related transporter genes. These expression pattern clusters should also represent a more robust source of insight than the LCI gene approach with regard to the role of CIA5 and CO₂ regulation on limiting CO₂ acclimation responses in general and on the function of the CCM specifically. An example of this is the indication, based on expression patterns observed with Calvin cycle genes and photorespiratory genes, that CIA5 may act as an upstream activator of photorespiratory genes and a mild upstream repressor of Calvin cycle genes. Thus, this study of transcriptome-wide patterns of gene expression related to CO₂ and CIA5 provides insight into the massive impact of these two factors and their interaction on gene expression in *C. reinhardtii*, in addition to identifying compelling new candidates for functional CCM components and highlighting new questions to be addressed in subsequent work.

METHODS

Chlamydomonas reinhardtii Strains and Culture Conditions

C. reinhardtii wild-type strain cc125 was obtained from the *Chlamydomonas* Resource Center (University of Minnesota, Minneapolis, MN). The *cia5* mutant (strain cc2702) was a gift from Donald P. Weeks (University of Nebraska, Lincoln, NE). Media and growth conditions for *C. reinhardtii* were described previously (Wang and Spalding, 2006). All strains were maintained on CO₂ minimal plates in high CO₂ (air enriched with 5% CO₂) chambers at room temperature, under continuous illumination (50 $\mu\text{mol photons m}^{-2} \text{s}^{-1}$). Liquid cultures were grown on a gyratory shaker (speed 200 rpm) under white light ($\sim 100 \mu\text{mol photons m}^{-2} \text{s}^{-1}$) at room temperature.

Induction and RNA Isolation

Liquid cultures of all strains were grown under H-CO₂ (5% [v/v] CO₂) to a concentration of 1.0 to 2.0 million cells per mL. Cell cultures were then equally distributed into nine flasks, with three flasks each aerated with H-CO₂ (5%), L-CO₂ (nominally 300 to ~ 500 ppm; actually 330 to 410 ppm), or VL-CO₂ (nominally 100 to ~ 200 ppm; actually 110 to 152 ppm). Selection of gas flow lines and position on the shaker were completely random. After 4 h induction, cultures aerated with the same CO₂ concentrations were combined and centrifuged to collect cells. Two biological replicates of each strain and of each induction condition were processed for RNA isolation as previously described (Wang and Spalding, 2006), and crude RNA samples were cleaned with DNase I and the RNeasy MinElute Cleanup kit (Qiagen).

Sequencing and Alignment

The DNA Facility at Iowa State University processed the cleaned RNA samples, prepared the libraries, and generated sequences (one sample per lane on the flow cell) on a Genome Analyzer II system (Illumina). No less than 12 million reads were obtained for each sample (details can be found in Supplemental Table 1 online). Raw and processed sequence files are available at the National Center for Biotechnology Information Gene Expression Omnibus (accession number GSE33927).

Raw reads were aligned to the version 4.0 assembly of the *C. reinhardtii* genome (<http://genome.jgi-psf.org/chlamy/chlamy.info.html>) using *gmap* (Wu and Watanabe, 2005), which tries to align every single read to the genome as an mRNA (possibly spliced) read without previous knowledge of the genome annotation or sequencing coverage. Alignment files were processed to retrieve unique alignments with an alignment score higher than $r-15$, where r is the read length. This choice allows us to (1) keep two-

block alignments (reads that span two different exons) where only one block is reported by *gmap* (that typically fails to provide alignment blocks smaller than 16 because of its indexing strategy) and (2) keep alignments for trimmed reads with sequencing errors at the 3' end. Only high-similarity (less than three mismatches) and intron-like alignments (defined here as those with up to one gap smaller than 5 kb) were used for expression estimation.

Counts per gene were estimated by requiring complete overlap between each alignment and the transcript genomic coordinates and after normalization of transcript sequence coverage by read length for each sample. This strategy attempts to remove the impact that different read lengths could have on the final results, but almost identical results were found with alternative methods (see the end of Methods). Augustus 5.0 gene models (<http://augustus.gobics.de/predictions/chlamydomonas/>) were used as the reference annotation in this work. The original annotation was filtered to keep only the first prediction for each locus ("_t1" transcripts). Total number of sequences, percentage of uniquely aligned reads, and total gene counts per sample are provided in Supplemental Table 1 online. Gene counts were used for differential expression analysis. Expression estimates for each sample are provided in units of RPKM (reads per kilobase of exon model per million of aligned reads; Mortazavi et al., 2008).

Normalization and Statistical Analysis

The primary statistical analysis was performed in the *R* statistical programming language (version 2.10.1 from <http://www.r-project.org/>). A generalized linear model with negative binomial distribution and logarithm link function was fitted to the counts of reads separately for each gene, while the sequencing depths were used as the offsets for normalization purpose. Fixed factors in the model included CO₂ condition, strain, and their interaction. An overall test was conducted to identify genes with differential expression in any of the six treatment groups. This test was performed by comparing the full model with six separate means and a reduced model with the same mean for all six groups using quasi-likelihood-based approach. The set of *P* values from the overall test for each gene was adjusted for FDR control as described by Benjamini and Hochberg (1995). For each of the genes identified as DE by the overall test while FDR was controlled at 2.5%, we further tested (C/S impact test) for CO₂ effect (C-effect), strain effect (S-effect), and CO₂ and strain interaction effect (CS-effect). These C/S impact tests were conducted by comparing the full model with the appropriate reduced models using quasi-likelihood-based *F*-test with the *R* function "*drop1*." FDR was controlled for each set of *P* values using Benjamini and Hochberg's method.

The DE genes identified by the overall test were clustered by a model-based clustering method implemented in an *R* package, *MBCluster.Seq* (Y. Si, P. Liu, P. Li, and T.P. Brutnell, unpublished, <http://www.stat.iastate.edu/preprint/articles/2011-11.pdf>), assuming the observed counts following negative binomial distributions. Results were evaluated for variations in the number of clusters from 10 to 30. To maintain the clusters as few and tight as possible while including most of the patterns, 16 was chosen to be the total number of clusters for further analysis by visual inspection of the clustering results.

Pairwise comparisons between VL-CO₂ and L-CO₂ states, VL-CO₂ and H-CO₂ states, or L-CO₂ and H-CO₂ states were performed using the Bioconductor package *DESeq* (Anders and Huber, 2010), which performs variance stabilization by borrowing information across genes (Anders and Huber, 2010). The set of *P* values for each test was adjusted for FDR control as described by Benjamini and Hochberg (1995).

Quantitative Real-Time PCR Analysis

SYBR green one-step quantitative PCR system was used for qPCR analysis (Quanta Biosciences). All experiments were performed on a Bio-

Rad iCycler iQ real-time PCR detection system using primers described in Supplemental Table 2 online. The RNA samples used as templates for qPCR were the same as those used for RNA-Seq. The CBLP gene was used as internal control for normalization of qPCR data. Pearson correlations were calculated for each gene across six strain treatment conditions between RNA-Seq and qPCR methods, based on average \log_2 fold change of two biological replicates.

Functional Categorization for DE Genes Using the Pathways Tool

The Algal Functional Annotation Tool (Lopez et al., 2011) was used to investigate the biological processes associated with each cluster. To address the limitation of annotations availability for *C. reinhardtii*, we used the GO terms based on orthology to *Arabidopsis thaliana* as the framework for GO term selection. After inputting the gene list for each cluster separately, P values were generated for each GO term for each cluster entry. GO terms lacking any hits were assigned a P value of 1, and other terms not statistically significant ($P > 0.01$) for any cluster entry were excluded in generating the summary heat map (see Supplemental Figure 7 online).

Manual Curation for DE Genes

The principles we followed when manually curating these genes were as follows: (1) manual annotation was used if available; (2) if there was no manual annotation, the automated annotation domain information based on the Augustus 5.0 gene model was used to guide curation of the gene; (3) if there was no manual annotation and no identified domains from the automated annotation, the gene was marked as “unknown,” or as “unknown transmembrane,” if one or more transmembrane regions were predicted; (4) any domain information provided by automated annotation of the gene models was used to place the genes into broad functional categories. The categories used included general biological pathways and general protein functions, such as “metabolism” or “signaling.” From this process, we placed all genes into eight general categories reflective of putative function: (1) signaling (including protein kinases, cyclic nucleotide synthesis, and metabolism, etc.); (2) gene expression and regulation (including transcription, translation, RNA processing, chromatin structure, and dynamics, etc.); (3) transport (including C_i transport, ion transport, and metabolite transport, etc.); (4) metabolism (including amino acid, photosynthesis, photorespiration, carbohydrate, acetate, lipid, and macronutrients, etc.); (5) stress and cell death (including oxidative stress, autophagy, and programmed cell death, etc.); (6) cell structure and function (including cell wall, cytoskeleton, vesicular trafficking, protein trafficking, cell division, and cell motility, etc.); (7) protein modification and regulation (including proteases and protein modifications other than kinases, etc.); and (8) unknown.

An Alternative RNA-Seq Data Evaluation for Reproducibility and Comparative Analysis

Here, we provide additional data regarding the quality and reproducibility of our RNA-Seq libraries, along with a comparative analysis with the results from our companion article (Bruggeman et al., 2012). To this end, we used a different, simplified pipeline for all data to highlight the biological differences and remove any potential differences due to the computational methods. Specifically, we performed the steps below.

- To remove any dependency with the various parameters involved in gapped-alignment algorithms, we first obtained nongapped alignments to Augustus 5 transcript sequences using *bowtie*. The potential issues introduced by this approach (slightly worse alignment rates and missing annotations in the genome with sequence similarity to the annotated genome) are not expected to make a difference in the expression and differential expression results for most genes.
- Trimming sequences: To remove the impact that different read length and error rates could have in comparing different RNA-Seq libraries, the results below correspond to trimmed libraries (60 bp) showing very similar error rate

profiles (around 1% at the 3' end; data not shown). The rate of unique alignment to Augustus 5 transcripts is in the range of 70 to 80% for all libraries (see Supplemental Table 1 online).

- Unique hits from *bowtie* were compiled to build the count matrix per gene per sample, for both our libraries and those from our companion article. The previous matrix was normalized to compute expression estimates in unit of RPKMs. This normalization was performed after imputation of missing values (0s were imputed a value of 1 count to regularize fold changes and differential expression estimates) and filtering those genes with no counts in any sequencing lane (absent or nonmappable genes).

Some remarks that can be made from these normalized values follow:

- High-expression tails: as normalized RPKM values provide relative expression measures, one of the main sources of ambiguity when comparing two different RNA-Seq data sets comes from the distribution of the high-expression genes. Very small changes in the high-expression tail of the distribution changes significantly the estimates for moderately and slightly expressed genes. As an example, we can compute the fraction of the total RPKMs corresponding to the top 100 highly expressed transcripts. For those conditions that are similar in both articles, the numbers are as follows: Fang/Spalding data set high CO_2 #1 = 0.4117; Fang/Spalding data set high CO_2 #2 = 0.4650; Fang/Spalding data set very low CO_2 #1 = 0.3849; Fang/Spalding data set very low CO_2 #2 = 0.4445; Bruggeman/Ladunga data set 0 h #1 = 0.4528; Bruggeman/Ladunga data set 0 h #2 = 0.5357; Bruggeman/Ladunga data set 3 h #1 = 0.6786; and Bruggeman/Ladunga data set 3 h #2 = 0.7031.

For instance, the last number means that 70% of the RPKMs come from the top 100 genes in the 3-h sample (second replicate) of the Bruggeman et al. (2012) data set. This observation, in its turn, will clearly impact the mean variance distributions so that the number of reported DE genes is potentially different. The biological interpretation of this difference in the expression distributions can be found in both articles and can be easily understood from the differences in experimental conditions and/or genetic background.

- Reproducibility. A high correlation between fold change estimates from both RNA-Seq and PCR is shown and discussed in this article for a number of relevant genes. Regarding the reproducibility of our RNA-Seq expression estimates for different replicates, Supplemental Figure 3 online shows mean difference scatterplots for replicates of the same condition in our article. The x axis values are geometric means of the expression of the two replicates, while the y axis shows the fold change between replicates. To assist with the visualization of these graphs, shown are line plots with the 90th percentile (red), mean (green), and 10th percentile (cyan) of the fold changes. This means that above the red line fall the 10% higher fold changes between replicates and below the cyan is the 10% higher negative fold changes between replicates. These plots show both that the replicates fold change distributions are centered around 0 as expected (green lines) and that the expression estimates from both replicates area consistent for a majority of the transcriptome. Very similar results were found for the experiments from our companion article (Bruggeman et al., 2012). It is worth mentioning that the highest reproducibility is observed for the mutant samples, most likely due to a lower sensitivity to fluctuations in CO_2 levels.
- Fold change comparative plots: Fold changes between control and experiment were obtained from the mean expression estimates across replicates for each condition. We focus here on those comparisons that are common to both articles (very low/high CO_2 for our data set and 0 versus 3 h on the Bruggeman et al. [2012] data set). Supplemental Figure 4 online compares both fold change estimates. The left panel shows a scatterplot along with results from a linear fit. The black line is a guide to the eye, representing an ideal linear relationship (slope = 1, no offset, expected if both experiments were completely equivalent). A linear fit provides the results highlighted in red font, with slope 1.13 and offset = -0.56. The correlation between both fold change distributions is 0.60. Together, these results indicate that both data sets have the same whole-transcriptome trends in fold expression. The same data are shown in the right panel of Supplemental Figure 4 online as a smoothed density

plot. It is clear that fold changes for a majority of genes are in close agreement between both data sets, in accordance with the discussion in the articles regarding the similarity between the reported regulated genes.

- Fold-change comparative plots for different analysis pipelines: Supplemental Figure 5 online shows scatterplots of \log_2 fold changes estimated for data in this article with two different analysis pipelines. The x axis corresponds to the fold change estimates presented in the main article, while the y axis plots estimates from the pipeline introduced above. Red lines represent a perfect linear relationship. The agreement between both estimates is apparent for the whole fold change dynamic range.

Accession Numbers

All sequence data from this article can be found in the GenBank/EMBL data libraries under accession numbers listed in Supplemental Data Set 2 online. Accession numbers for specifically discussed genes are as follows: *AAT1*, EDP08011; *AGT1*, EDO97315; *AGT2*, EDO96807; *CAH1*, EDP04241; *CAH3*, EDP00852; *CAH4*, EDO96058; *CAH5*, EDP07024; *CAH6*, EDO96552; *CAH7*, EDO99006; *CAH8*, EDO99999; *CAH9*, EDP07163; *CCM1/CIA5*, EDP07542; *CCP1*, EDP04147; *CCP2*, EDP04238; *DLDH1*, EDP01871; *DNJ15*, EDP03107; *DNJ31*, EDO98634; *FBA1*, EDO98285; *FBA3*, EDO97897; *FBP1*, EDP05318; *GCSH*, EDP08614; *GLYK*, EDP03009; *GYD1*, EDP01639; *HLA3*, EDP07736; *HPR1*, EDP05213; *LCI1*, EDP06069; *LCI6*, EDP02960; *LCIA/NAR1.2*, EDP04946; *LCIB*, EDP07837; *LCIC*, EDP04956; *LCID*, EDP04142; *LCIE*, EDP04243; *LCR1*, BAD13492; *LHCSR2*, EDP01013; *LHCSR3*, EDP01087; *PGK1*, EDO98586; *PGP1*, EDP06184; *PGP2*, EDP05829; *PGP3*, EDP08194; *PRK1*, EDP02974; *RBCS1*, EDO96904; *RHP1*, EDP01722; *RHP2*, EDP01723; *RPI1*, EDP04506; *SEBP1*, EDP04487; *SGA1*, EDO97196; *SHMT1*, EDO97448; *SHMT2*, EDO97351; and *SHMT3*, EDP00905. *C. reinhardtii* strains (available from the *Chlamydomonas* Stock Center; <http://chlamycollection.org/>) used in this work are as follows: the 137c wild type (strain cc125) and the *cia5* mutant (strain cc2702).

Supplemental Data

The following materials are available in the online version of this article.

Supplemental Figure 1. Gene Expression Level Distributions for Each Treatment Condition.

Supplemental Figure 2. Validation of RNA-Seq by qPCR.

Supplemental Figure 3. Mean Difference Scatterplots for Biological Replicates.

Supplemental Figure 4. Comparison of \log_2 Fold Change Estimates between Different Data Sets.

Supplemental Figure 5. Comparison of \log_2 Fold Change Estimates between Different Analysis Pipelines.

Supplemental Figure 6. Distribution of C/S Impact Test Results by Cluster.

Supplemental Figure 7. Heat Map for GO Category Hits Based on the Algal Functional Annotation Tool.

Supplemental Table 1. Alignment Statistics for the Transcriptome Sequencing Experiment.

Supplemental Table 2. List of qPCR Primers.

Supplemental Data Set 1. Overall and C/S Impact Test.

Supplemental Data Set 2. DESeq Summary.

Supplemental Data Set 3. Gene Ontology Analysis.

Supplemental Data Set 4. Manual Curation of Genes.

Supplemental Data Set 5. Previously Reported LCI Genes.

Supplemental Data Set 6. Genes in CCM clusters 8, 14, and 15.

ACKNOWLEDGMENTS

This work was supported by USDA National Research Initiative Competitive grants (2007-35318-18433), by the National Science Foundation (MCB-0952323), and by the Department of Energy Advanced Research Projects Agency-Energy Program (DEAR0000010) to M.H.S., as well as by the Institute of Genomics and Proteomics (Department of Energy Cooperative Agreement DE-FC02-02ER63421 to David Eisenberg) and the National Institutes of Health (R24GM092473) to S.S.M. and M.H.P.

AUTHOR CONTRIBUTIONS

W.F., P.L., and M.H.S. designed the research. W.F. performed the research. Y.S. and P.L. contributed new analytical tools. All authors analyzed data, and all authors contributed to the writing of the article.

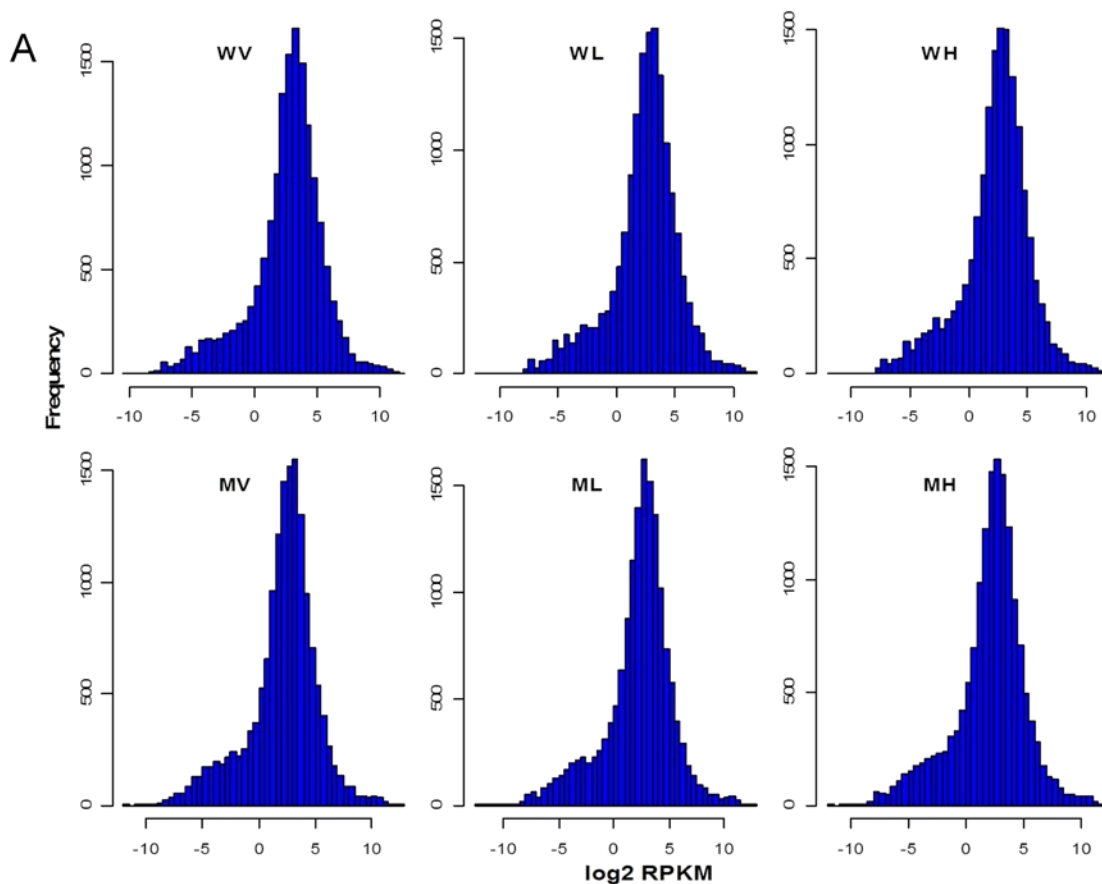
Received March 12, 2012; revised March 12, 2012; accepted May 14, 2012; published May 25, 2012.

REFERENCES

- Anders, S., and Huber, W. (2010). Differential expression analysis for sequence count data. *Genome Biol.* **11**: R106.
- Andersson, I. (2008). Catalysis and regulation in Rubisco. *J. Exp. Bot.* **59**: 1555–1568.
- Benjamini, Y., and Hochberg, Y. (1995). Controlling the false discovery rate: A practical and powerful approach to multiple testing. *J. R. Stat. Soc. B* **57**: 289–300.
- Brueggeman, A.J., Gangadharaiah, D.S., Cserhati, M.F., Casero, D., Weeks, D.P., and Ladunga, I. (2012). Activation of the carbon-concentrating mechanism by CO₂ deprivation coincides with massive transcriptional and metabolic restructuring in *Chlamydomonas reinhardtii*. *Plant Cell* **24**: 1860–1875.
- Castruita, M., Casero, D., Karpowicz, S.J., Kropat, J., Vieler, A., Hsieh, S.I., Yan, W., Cokus, S., Loo, J.A., Benning, C., Pellegrini, M., and Merchant, S.S. (2011). Systems biology approach in *Chlamydomonas* reveals connections between copper nutrition and multiple metabolic steps. *Plant Cell* **23**: 1273–1292.
- Chen, Z.-Y., Burow, M.D., Mason, C.B., and Moroney, J.V. (1996). A low-CO₂-inducible gene encoding an alanine: alpha-ketoglutarate aminotransferase in *Chlamydomonas reinhardtii*. *Plant Physiol.* **112**: 677–684.
- Chen, Z.Y., Lavigne, L.L., Mason, C.B., and Moroney, J.V. (1997). Cloning and overexpression of two cDNAs encoding the low-CO₂-inducible chloroplast envelope protein LIP-36 from *Chlamydomonas reinhardtii*. *Plant Physiol.* **114**: 265–273.
- Coleman, J.R., and Grossman, A.R. (1984). Biosynthesis of carbonic anhydrase in *Chlamydomonas reinhardtii* during adaptation to low CO₂. *Proc. Natl. Acad. Sci. USA* **81**: 6049–6053.
- Dillard, S.R., Van, K., and Spalding, M.H. (2011). Acclimation to low or limiting CO₂ in non-synchronous *Chlamydomonas* causes a transient synchronization of the cell division cycle. *Photosynth. Res.* **109**: 161–168.
- Duanmu, D., Miller, A.R., Horken, K.M., Weeks, D.P., and Spalding, M.H. (2009a). Knockdown of limiting-CO₂-induced gene *HLA3* decreases HCO₃⁻ transport and photosynthetic Ci affinity in *Chlamydomonas reinhardtii*. *Proc. Natl. Acad. Sci. USA* **106**: 5990–5995.

- Duanmu, D., Wang, Y., and Spalding, M.H. (2009b). Thylakoid lumen carbonic anhydrase (CAH3) mutation suppresses air-Dier phenotype of *LCIB* mutant in *Chlamydomonas reinhardtii*. *Plant Physiol.* **149**: 929–937.
- Fukuzawa, H., Miura, K., Ishizaki, K., Kucho, K.I., Saito, T., Kohinata, T., and Ohya, K. (2001). *Ccm1*, a regulatory gene controlling the induction of a carbon-concentrating mechanism in *Chlamydomonas reinhardtii* by sensing CO₂ availability. *Proc. Natl. Acad. Sci. USA* **98**: 5347–5352.
- Galván, A., Rexach, J., Mariscal, V., and Fernández, E. (2002). Nitrite transport to the chloroplast in *Chlamydomonas reinhardtii*: Molecular evidence for a regulated process. *J. Exp. Bot.* **53**: 845–853.
- González-Ballester, D., Casero, D., Cokus, S., Pellegrini, M., Merchant, S.S., and Grossman, A.R. (2010). RNA-seq analysis of sulfur-deprived *Chlamydomonas* cells reveals aspects of acclimation critical for cell survival. *Plant Cell* **22**: 2058–2084.
- Kvam, V.M., Liu, P., and Si, Y. (2012). A comparison of statistical methods for detecting differentially expressed genes from RNA-seq data. *Am. J. Bot.* **99**: 248–256.
- Lopez, D., Casero, D., Cokus, S.J., Merchant, S.S., and Pellegrini, M. (2011). Algal Functional Annotation Tool: A web-based analysis suite to functionally interpret large gene lists using integrated annotation and expression data. *BMC Bioinformatics* **12**: 282.
- Marek, L.F., and Spalding, M.H. (1991). Changes in photorespiratory enzyme activity in response to limiting CO₂ in *Chlamydomonas reinhardtii*. *Plant Physiol.* **97**: 420–425.
- Mariscal, V., Moulin, P., Orsel, M., Miller, A.J., Fernández, E., and Galván, A. (2006). Differential regulation of the *Chlamydomonas* *Nar1* gene family by carbon and nitrogen. *Protist* **157**: 421–433.
- Mitra, M., Lato, S.M., Ynalvez, R.A., Xiao, Y., and Moroney, J.V. (2004). Identification of a new chloroplast carbonic anhydrase in *Chlamydomonas reinhardtii*. *Plant Physiol.* **135**: 173–182.
- Miura, K., Yamano, T., Yoshioka, S., Kohinata, T., Inoue, Y., Taniguchi, F., Asamizu, E., Nakamura, Y., Tabata, S., Yamato, K.T., Ohya, K., and Fukuzawa, H. (2004). Expression profiling-based identification of CO₂-responsive genes regulated by CCM1 controlling a carbon-concentrating mechanism in *Chlamydomonas reinhardtii*. *Plant Physiol.* **135**: 1595–1607.
- Moroney, J.V., Husic, H.D., Tolbert, N.E., Kitayama, M., Manuel, L.J., and Togasaki, R.K. (1989). Isolation and characterization of a mutant of *Chlamydomonas reinhardtii* deficient in the CO₂ concentrating mechanism. *Plant Physiol.* **89**: 897–903.
- Moroney, J.V., Ma, Y., Frey, W.D., Fusilier, K.A., Pham, T.T., Simms, T.A., DiMario, R.J., Yang, J., and Mukherjee, B. (2011). The carbonic anhydrase isoforms of *Chlamydomonas reinhardtii*: Intracellular location, expression, and physiological roles. *Photosynth. Res.* **109**: 133–149.
- Moroney, J.V., and Ynalvez, R.A. (2007). Proposed carbon dioxide concentrating mechanism in *Chlamydomonas reinhardtii*. *Eukaryot. Cell* **6**: 1251–1259.
- Mortazavi, A., Williams, B.A., McCue, K., Schaeffer, L., and Wold, B. (2008). Mapping and quantifying mammalian transcriptomes by RNA-Seq. *Nat. Methods* **5**: 621–628.
- Ohnishi, N., Mukherjee, B., Tsujikawa, T., Yanase, M., Nakano, H., Moroney, J.V., and Fukuzawa, H. (2010). Expression of a low CO₂-inducible protein, LCI1, increases inorganic carbon uptake in the green alga *Chlamydomonas reinhardtii*. *Plant Cell* **22**: 3105–3117.
- Pollock, S.V., Prout, D.L., Godfrey, A.C., Lemaire, S.D., and Moroney, J.V. (2004). The *Chlamydomonas reinhardtii* proteins Ccp1 and Ccp2 are required for long-term growth, but are not necessary for efficient photosynthesis, in a low-CO₂ environment. *Plant Mol. Biol.* **56**: 125–132.
- Ramazanov, Z., Mason, C.B., Geraghty, A.M., Spalding, M.H., and Moroney, J.V. (1993). The low CO₂-inducible 36-kilodalton protein is localized to the chloroplast envelope of *Chlamydomonas reinhardtii*. *Plant Physiol.* **101**: 1195–1199.
- Raven, J.A., Cockell, C.S., and De La Rocha, C.L. (2008). The evolution of inorganic carbon concentrating mechanisms in photosynthesis. *Philos. Trans. R. Soc. Lond. B Biol. Sci.* **363**: 2641–2650.
- Somanchi, A., and Moroney, J.V. (1999). As *Chlamydomonas reinhardtii* acclimates to low-CO₂ conditions there is an increase in cyclophilin expression. *Plant Mol. Biol.* **40**: 1055–1062.
- Soupe, E., Inwood, W., and Kustu, S. (2004). Lack of the Rhesus protein Rh1 impairs growth of the green alga *Chlamydomonas reinhardtii* at high CO₂. *Proc. Natl. Acad. Sci. USA* **101**: 7787–7792.
- Soupe, E., King, N., Feild, E., Liu, P., Niyogi, K.K., Huang, C.H., and Kustu, S. (2002). Rhesus expression in a green alga is regulated by CO₂. *Proc. Natl. Acad. Sci. USA* **99**: 7769–7773.
- Spalding, M.H. (2008). Microalgal carbon-dioxide-concentrating mechanisms: *Chlamydomonas* inorganic carbon transporters. *J. Exp. Bot.* **59**: 1463–1473.
- Spalding, M.H. (2009). CO₂-concentrating mechanism and carbon assimilation. In *The Chlamydomonas Sourcebook: Organellar and Metabolic Processes*, 2nd ed, Vol. 2, D. Stern and E. Harris, eds (Amsterdam: Elsevier Publishers), pp. 257–301.
- Spalding, M.H., and Jeffrey, M. (1989). Membrane-associated polypeptides induced in *Chlamydomonas* by limiting CO₂ concentrations. *Plant Physiol.* **89**: 133–137.
- Spalding, M.H., Spreitzer, R.J., and Ogren, W.L. (1983a). Carbonic anhydrase-deficient mutant of *Chlamydomonas reinhardtii* requires elevated carbon dioxide concentration for photoautotrophic growth. *Plant Physiol.* **73**: 268–272.
- Spalding, M.H., Spreitzer, R.J., and Ogren, W.L. (1983b). Reduced inorganic carbon transport in a CO₂-requiring mutant of *Chlamydomonas reinhardtii*. *Plant Physiol.* **73**: 273–276.
- Spalding, M.H., Van, K., Wang, Y., and Nakamura, Y. (2002). Acclimation of *Chlamydomonas* to changing carbon availability. *Funct. Plant Biol.* **29**: 221–230.
- Tural, B., and Moroney, J.V. (2005). Regulation of the expression of photorespiratory genes in *Chlamydomonas reinhardtii*. *Can. J. Bot.* **83**: 810–819.
- Wang, L., Li, P., and Brutnell, T.P. (2010). Exploring plant transcriptomes using ultra high-throughput sequencing. *Brief Funct. Genomics* **9**: 118–128.
- Wang, Y., Duanmu, D., and Spalding, M.H. (2011). Carbon dioxide concentrating mechanism in *Chlamydomonas reinhardtii*: Inorganic carbon transport and CO₂ recapture. *Photosynth. Res.* **109**: 115–122.
- Wang, Y., and Spalding, M.H. (2006). An inorganic carbon transport system responsible for acclimation specific to air levels of CO₂ in *Chlamydomonas reinhardtii*. *Proc. Natl. Acad. Sci. USA* **103**: 10110–10115.
- Wang, Y., Sun, Z., Horken, K.M., Im, C.S., Xiang, Y., Grossman, A.R., and Weeks, D.P. (2005). Analyses of CIA5, the master regulator of the carbon-concentrating mechanism in *Chlamydomonas reinhardtii*, and its control of gene expression. *Can. J. Bot.* **83**: 765–779.
- Wu, T.D., and Watanabe, C.K. (2005). GMAP: A genomic mapping and alignment program for mRNA and EST sequences. *Bioinformatics* **21**: 1859–1875.
- Xiang, Y., Zhang, J., and Weeks, D.P. (2001). The *Cia5* gene controls formation of the carbon concentrating mechanism in *Chlamydomonas reinhardtii*. *Proc. Natl. Acad. Sci. USA* **98**: 5341–5346.

- Yamano, T., and Fukuzawa, H.** (2009). Carbon-concentrating mechanism in a green alga, *Chlamydomonas reinhardtii*, revealed by transcriptome analyses. *J. Basic Microbiol.* **49**: 42–51.
- Yamano, T., Tsujikawa, T., Hatano, K., Ozawa, S.I., Takahashi, Y., and Fukuzawa, H.** (2010). Light and low-CO₂-dependent LCIB-LCIC complex localization in the chloroplast supports the carbon-concentrating mechanism in *Chlamydomonas reinhardtii*. *Plant Cell Physiol.* **51**: 1453–1468.
- Yoshihara, C., Inoue, K., Schichnes, D., Ruzin, S., Inwood, W., and Kustu, S.** (2008). An Rh1-GFP fusion protein is in the cytoplasmic membrane of a white mutant strain of *Chlamydomonas reinhardtii*. *Mol. Plant* **1**: 1007–1020.
- Yoshioka, S., Taniguchi, F., Miura, K., Inoue, T., Yamano, T., and Fukuzawa, H.** (2004). The novel Myb transcription factor LCR1 regulates the CO₂-responsive gene *Cah1*, encoding a periplasmic carbonic anhydrase in *Chlamydomonas reinhardtii*. *Plant Cell* **16**: 1466–1477.



B

Percentiles	WV	WL	WH	MV	ML	MH	average
5th	0.052	0.046	0.045	0.036	0.036	0.036	0.050
median	7.559	6.393	6.085	5.685	6.114	5.412	6.602
95th	90.893	89.327	89.106	79.273	83.608	82.291	85.495

Supplemental Figure 1. Gene expression level distributions for each treatment condition.

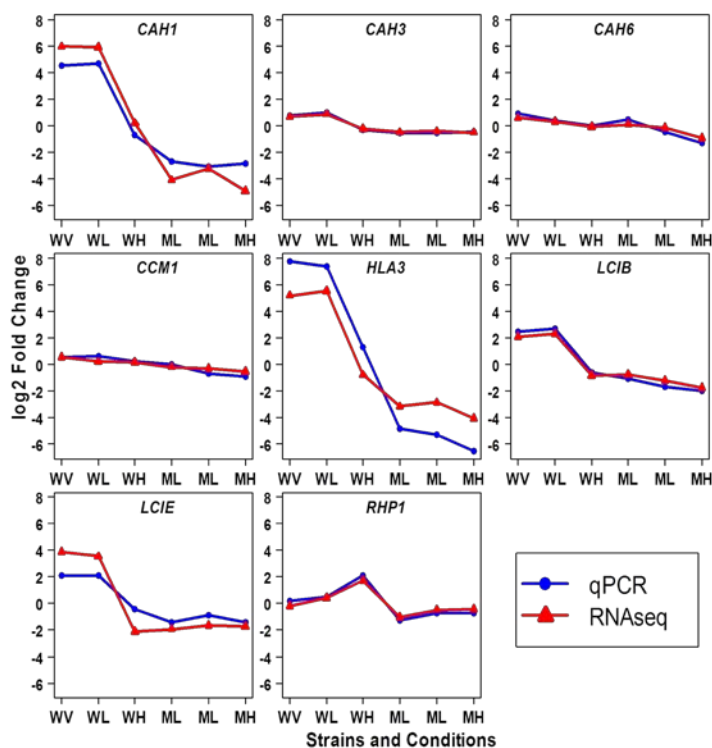
(A) The expression RPKM values are averaged between replicates under each treatment condition, then transformed by logarithm base 2. The title of each histogram indicates each strain and CO₂ treatment condition: WV = wild type under VL-CO₂ induction; WL = wild type under L-CO₂ induction; WH = wild type under H-CO₂ induction; MV = *cia5* under VL-CO₂ induction; ML = *cia5* under L-CO₂ induction; MH = *cia5* under H-CO₂ induction. The shapes of these distributions are very similar among all 6 conditions.

(B) This table summarizes the untransformed RPKMs' 5th, 50th, and 95th percentiles for each treatment condition and the average across conditions; these values are relatively consistent among all 6 treatment conditions.

A

Protein ID	Name	Correlation
522126	CAH1	0.98555
526413	CAH3	0.994444
512520	CAH6	0.970274
518901	CCM1	0.921299
518934	HLA3	0.980099
510298	LCIB	0.995218
522129	LCIE	0.968522
523557	RHP1	0.981095

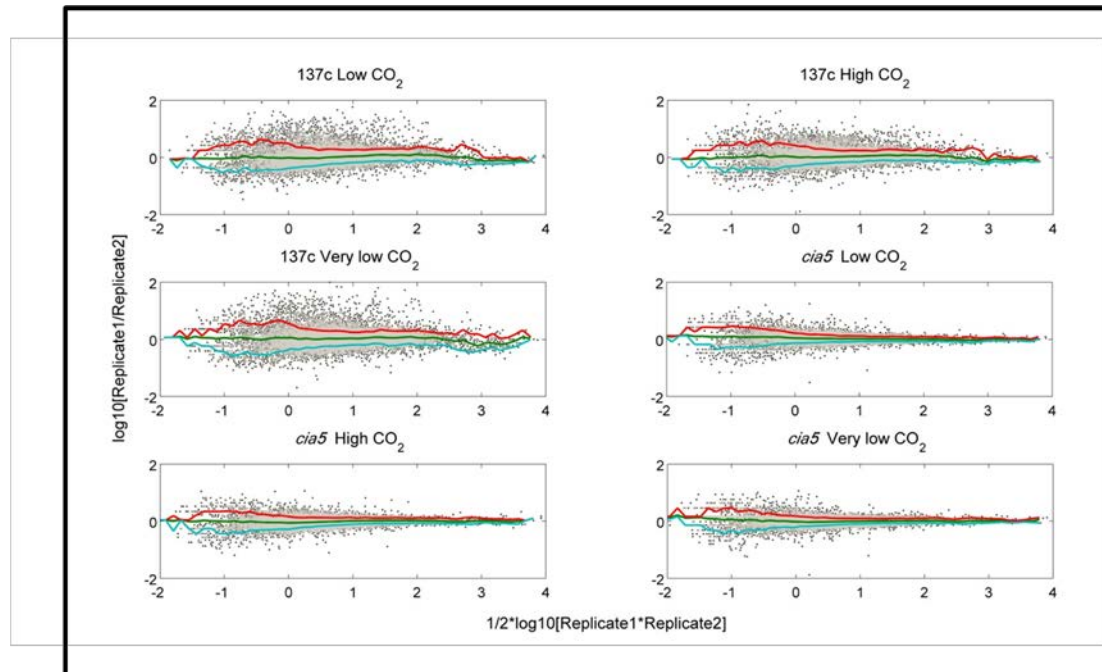
B



Supplemental Figure 2. Validation of RNA-Seq by qPCR.

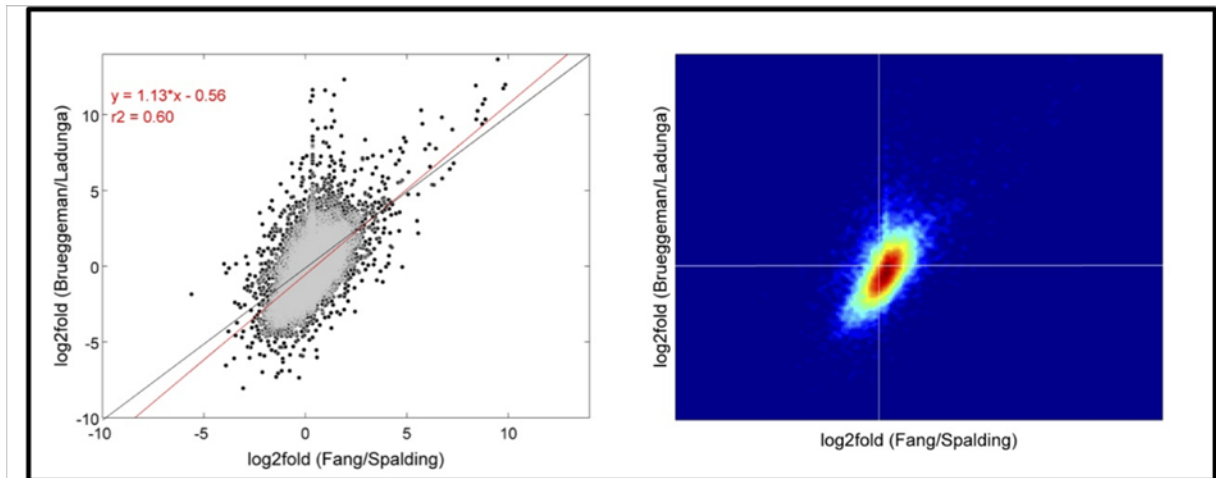
(A) Correlation coefficients between RNA-Seq and qPCR results for each of 8 genes. The correlation coefficients were calculated based on the \log_2 Fold Change of each individual condition relative to the overall mean across six conditions from the normalized RNA-Seq data and relative fold change values from the normalized qPCR data.

(B) Relative \log_2 Fold Change plot for selected genes. Horizontal axis indicates each strain and CO_2 induction condition: WV = wild type under VL- CO_2 induction; WL = wild type under L- CO_2 induction; WH = wild type under H- CO_2 induction; MV = *cia5* under VL- CO_2 induction; ML = *cia5* under L- CO_2 induction; MH = *cia5* under H- CO_2 induction. Red lines and blue lines separately represent RNA-Seq and qPCR relative \log_2 fold, and the closeness of the two lines visually illustrates the agreement between the 2 techniques.



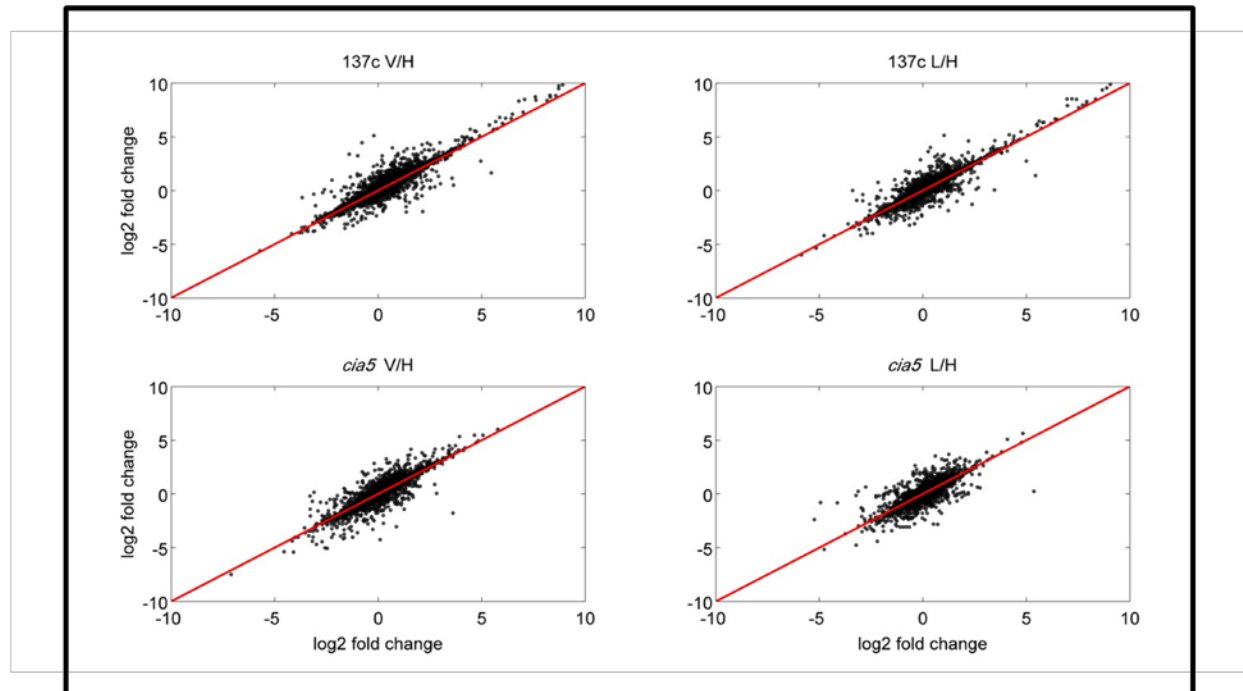
Supplemental Figure 3. Mean-difference scatter plots for biological replicates.

For each experiment, the log-log plot represents the fold change (y-axis) as a function of the geometric mean (x-axis), for each pair of replicates of the same experiment. Quantile line plots in running windows on the x-axis represent the 90th (red), mean (green) and 10th (cyan) quantile of the fold changes. In all cases it can be seen that the mean fold change is around 0 (green line) and a majority of genes show high correlation between different replicates, across most of the dynamic range of the mean expression.



Supplemental Figure 4. Comparison of log₂ fold change estimates between different datasets.

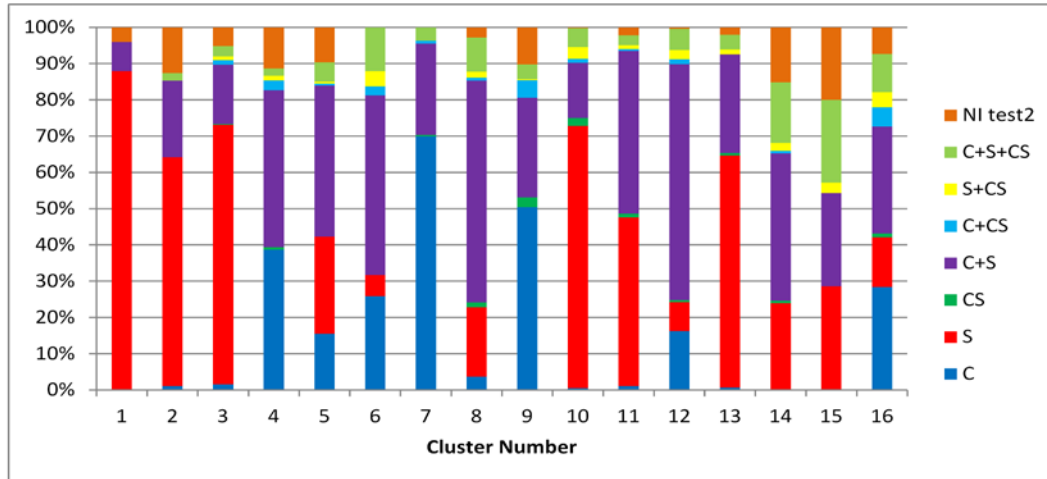
Left: log₂ fold changes of 3 hours after CO₂ deprivation from our companion paper (Brueggeman et al. 2012) are plotted against our fold changes estimates of very low versus high CO₂. A perfect linear relationship is represented with a black line, and the results from a linear fit are highlighted in red. Right: a density histogram of the same data is plotted to show that a majority of fold change estimates are in agreement between both datasets.



Supplemental Figure 5. Comparison of log₂ fold change estimates between different analysis pipelines.

Each panel compares log₂ fold change estimates as presented in the manuscript (x axis) to those obtained from an alternative, simplified pipeline on trimmed sequences (see Supplementary Data Methods). For each strain (137c, *cia5*), shown are log₂ fold changes of very low vs. high CO₂ (V/H) and low vs. high CO₂ (L/H).

A



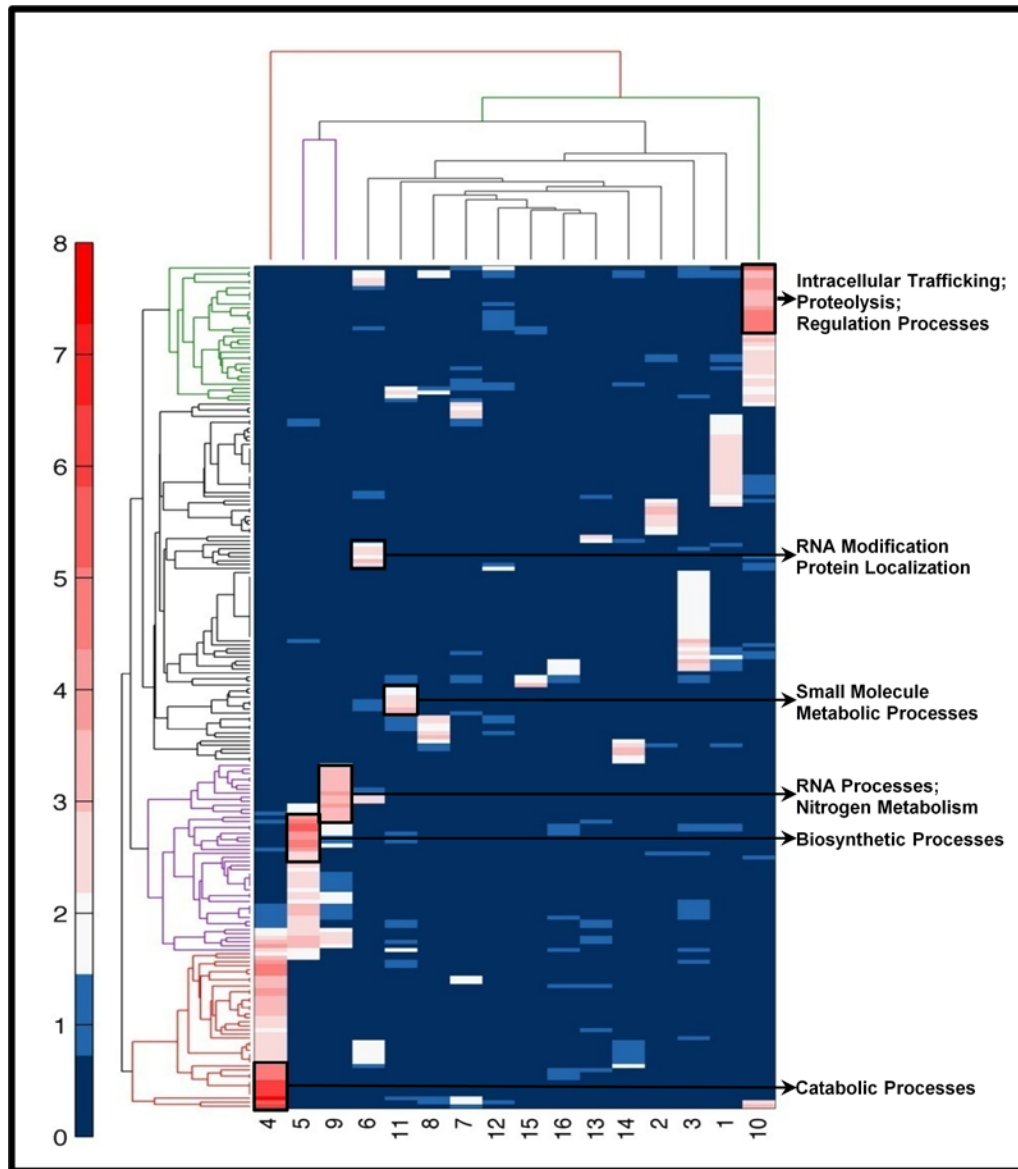
B

Significant effects	Total genes	For each Cluster															
		1	2	3	4	5	6	7	8	9	10	11	12	13	14	15	16
C	633	0	1	6	58	29	62	170	13	187	2	2	75	1	0	0	27
S	1184	109	60	277	0	50	14	0	69	0	333	85	37	94	33	10	13
CS	36	0	0	1	1	0	0	1	5	10	10	2	3	1	1	0	1
C+S	1324	10	20	63	65	78	119	61	220	102	70	82	301	40	56	9	28
C+CS	57	0	0	5	4	1	6	2	3	18	5	1	6	0	1	0	5
S+CS	63	0	0	4	2	1	10	0	6	1	15	2	12	2	3	1	4
C+S+CS	216	0	2	11	3	10	29	9	34	15	24	5	27	6	23	8	10
NI test2	165	5	12	20	17	18	0	0	10	38	1	4	2	3	21	7	7
total C	2230	10	23	85	130	118	216	242	270	322	101	90	409	47	80	17	70
total S	2787	119	82	355	70	139	172	70	329	118	442	174	377	142	115	28	55
total CS	372	0	2	21	10	12	45	12	48	44	54	10	48	9	28	9	20
total	3678	124	95	387	150	187	240	243	360	371	460	183	463	147	138	35	95

Supplemental Figure 6. Distribution of C/S impact test results by cluster.

(A) C/S impact test results for genes identified by the overall test as DE genes and clustered in 16 clusters. Cluster number is indicated on the horizontal axis, and the vertical axis indicates the percentage sum for significant individual effects, where significant = means $q\text{-value} < 0.025$. Different colors indicate specific individual effects or combinations as: C = significant CO₂ effect only; S = significant strain effect only; CS = significant strain and CO₂ interaction effect only; C+S = significant CO₂ and strain effect only; C+CS, significant CO₂ and interaction effect only; S+CS = significant strain and interaction effect only; C+S+CS = all 3 effects are significant; NI test2 = no significant effects in the C/S impact test but identified as a DE gene in the general test.

(B) Summary of the quantitative details for genes in the C/S impact test. The first column lists all combinations of significant individual effects; Total C, Total S or Total CS = all genes with indicated effect, including genes having either or both of the other individual effects. Totals are shown for all genes, as well as totals for each cluster.



Supplemental Figure 7. Heat map for GO category hits based on the Algal Functional Annotation Tool.

The heat map summarizes the Gene Ontology (GO) analysis results in the category of Biological Processes. GO terms and gene clusters were subjected to hierarchical clustering so that gene clusters with common significant ($p < 0.01$) ontology terms are placed close to each other in the tree for clearer illustration. Color schemes are indicated by the left vertical bar, where the numbers show the scale of negative logarithm of p -values. As a guide, darker in red means higher statistical significance for GO terms enriched in each cluster. Missing GO terms in any given cluster were assigned a p -value of 1. The almost complete absence of common GO hits between different clusters verifies the functional specificity of our gene clusters. Some highly enriched functional categories for specific clusters are highlighted as examples. Full details and enrichment p -values are provided in Supplemental Data Set 3 and discussed in the text.

Supplemental Table 1. Alignment Statistics for the transcriptome sequencing experiment.

Condition and replicate	Total Reads	Read Length	Uniquely Aligned (%)	Uniquely Aligned to AU5 Models	Uniquely Aligned to AU5 Models (%)
H-137c #1	14619355	75	92.5	10896815	74.54%
H-137c #2	13479946	80	93.0	10661929	79.09%
L-137c #1	13777581	75	92.6	10159785	73.74%
L-137c #2	12671440	80	92.9	10023000	79.10%
VL-137c #1	12228767	75	90.3	9749032	79.72%
VL-137c #2	12040923	80	93.1	7982253	66.29%
H- <i>cia5</i> #1	14659855	75	91.0	11199868	76.40%
H- <i>cia5</i> #2	15759589	83	93.0	12191567	77.36%
L- <i>cia5</i> #1	13574874	75	92.0	9464649	69.72%
L- <i>cia5</i> #2	18051524	83	92.6	15124925	83.79%
VL- <i>cia5</i> #1	15234796	75	91.7	11410522	74.90%
VL- <i>cia5</i> #2	19956363	83	93.0	15364398	76.99%

“Condition and replicate” column lists all RNA samples sequenced in this article: “H”, “L”, and “VL” are the CO₂ conditions; “137c” and “cia5” are the two strains we used in this experiment; “#1” or “#2” indicate the first or second biological replicate. “AU5 model” is the Augustus 5.0 gene model.

Supplemental Table 2. List of qPCR primers.

Augustus 5.0 Protein ID	Gene Name	Primer pair sequences
522126	<i>CAH1</i>	5' TCCTGGACGGGAAGGGTT 3' 5' CGATGCGGTTGGTCTGGTT 3'
526413	<i>CAH3</i>	5' AACCTGGCGTTCATTGGC 3' 5' CCTTGGGCGAGGGCTT 3'
512520	<i>CAH6</i>	5' TCTGGAGTATGCCGTGCTT 3' 5' TTGGCGCTCATGCTGTT 3'
518901	<i>CIA5/CCM1</i>	5' GGTCACGATGCGTCATTAGCG 3' 5' CAAGTGGTCCCTGTGATGCTCC 3'
518934	<i>HLA3</i>	5' CTCCGAGCGTCGTCTTTGTT 3' 5' TCGGCGTTCAGCTCCTCA 3'
510298	<i>LCIB</i>	5' TCACTGGTGACAACACCATCGC 3' 5' TGTTGAACGAGGAGCCGAAGATG 3'
522129	<i>LCIE</i>	5' AGCTACGTGGTGGTGAACGG 3' 5' TCATCATGTACTTGCGAGGGAT 3'
523557	<i>RHP1</i>	5' TTCGGAGCCTACTACGGATTG 3' 5' GCCTTCTTGGCATCGGTC 3'
514942	<i>CBLP</i>	5' ATGTGCTGTCCGTGGCTTTC 3' 5' CAGACCTTGACCATCTTGTCCC 3'

Transcriptome-Wide Changes in *Chlamydomonas reinhardtii* Gene Expression Regulated by Carbon Dioxide and the CO₂-Concentrating Mechanism Regulator *CIA5/CCM1*

Wei Fang, Yaqing Si, Stephen Douglass, David Casero, Sabeeha S. Merchant, Matteo Pellegrini, Istvan Ladunga, Peng Liu and Martin H. Spalding
Plant Cell 2012;24;1876-1893; originally published online May 25, 2012;
DOI 10.1105/tpc.112.097949

This information is current as of July 21, 2012

Supplemental Data	http://www.plantcell.org/content/suppl/2012/05/24/tpc.112.097949.DC2.html http://www.plantcell.org/content/suppl/2012/05/22/tpc.112.097949.DC1.html
References	This article cites 47 articles, 33 of which can be accessed free at: http://www.plantcell.org/content/24/5/1876.full.html#ref-list-1
Permissions	https://www.copyright.com/ccc/openurl.do?sid=pd_hw1532298X&issn=1532298X&WT.mc_id=pd_hw1532298X
eTOCs	Sign up for eTOCs at: http://www.plantcell.org/cgi/alerts/ctmain
CiteTrack Alerts	Sign up for CiteTrack Alerts at: http://www.plantcell.org/cgi/alerts/ctmain
Subscription Information	Subscription Information for <i>The Plant Cell</i> and <i>Plant Physiology</i> is available at: http://www.aspb.org/publications/subscriptions.cfm